



AFFIDAVIT

I declare that I have authored this thesis independently, that I have not used other than the declared sources/resources, and that I have explicitly indicated all material which has been quoted either literally or by content from the sources used. The text document uploaded to TUGRAZonline is identical to the present master's thesis.

Date

Signature

ACKNOWLEDGMENTS

At first I would like to express my sincere gratitude to Karl Lohner for giving me the chance to do my master thesis in this experienced group and Nermina Malanovic, who introduced me to the topic and all the working procedure. They supervised me throughout my time as their master student and always had time for me, whenever I had a question about my research or writing. I could not have imagined having better supervisors for my master thesis.

Besides my supervisors, I want to thank Dagmar Zweytick, Sabrina Riedl and Alexandra Zenz for helping me every time I needed something.

I also want to thank my colleagues for their discussions and the pleasant atmosphere.

Furthermore, I am grateful to all my friends for their continuous encouragement before and during my study.

Last but not least I want to thank my parents and my sister for supporting me during my thesis and my whole life, believing in me and always being on my side.

I will be grateful forever for your love!

TABLE OF CONTENTS

ABSTRACT	1
ZUSAMMENFASSUNG	3
I. INTRODUCTION	5
1. The problem of antibiotic resistance	5
2. Antimicrobial peptides	6
3. Biological cell membranes	7
4. Phospholipids	9
5. Human cathelicidin LL-37, an antimicrobial peptide	11
6. Antimicrobial peptides used in this thesis: OP-145, P148 and I12K	12
II. MATERIALS AND METHODS	15
1. Peptides	15
2. Lipids.....	15
3. Preparation of liposomes	16
4. Differential Scanning Calorimetry (DSC)	17
5. Phosphate determination	18
6. Fluorescence spectroscopy and leakage assay	19
7. Bacterial strains and growing conditions	20
8. Antimicrobial activity.....	20
9. Membrane permeabilization using living bacteria by flow cytometry.....	21
10. Fluorescence Microscopy	22

III.RESULTS	24
1. Antimicrobial activity.....	24
2. Membrane permeabilization.....	26
2.1 Permeabilization of living <i>E. coli</i> cells.....	26
2.2 Permeabilization of model membranes mimicking bacterial membrane composition...	30
3. Interaction with Gram-negative bacterial model membranes	31
3.1 Thermodynamic studies with model membranes composed of phospholipids with saturated fatty acids	32
3.2 Thermodynamic studies with model membranes composed of phospholipids with (un)saturated fatty acids.....	35
4. Lipid domain formation <i>in vivo</i> induced by AMPs	38
IV.DISCUSSION	41
ABBREVIATIONS	48
REFERENCES	50

ABSTRACT

The increase of antibiotic resistant pathogens represents a global health problem and therefore it is necessary to find therapeutic agents with novel mechanisms of action. Antimicrobial peptides (AMPs) which are part of the innate immune system of many diverse species are valuable template structures for the development of such agents. They efficiently kill bacterial pathogens within minutes primarily via membrane damage. The permeabilization of cellular envelopes is strongly affected by the lipid composition of the plasma membrane, which varies between mammals and bacteria. Such cationic and amphipathic peptides show a high activity against negatively charged bacterial membranes.

The focus of this project was to correlate the antimicrobial activity of three AMPs derived from the human cathelicidin LL-37 with membrane permeabilization of Gram-negative bacterial strains such as *Escherichia coli* ATCC 25922 and *Escherichia coli* K12 5K as well as of model membranes mimicking the inner membrane of Gram-negative bacterial cells. The investigated peptides OP-145, P148 and I12K with a length of 24 amino acids adopt an α -helical structure. They interact preferentially with the negatively charged phosphatidylglycerol (PG) leading to a disordering of the membrane.

P148 showed the highest activity against both *E. coli* strains reaching the lethal concentration (LC_{99.9}) after 5 minutes at 0.8 μ M. Whereas OP-145 shows reduced but similar activity against the two strains, the peptide I12K has a different lethal concentration depending on the *E. coli* strain. Real-time measurements of membrane permeabilization showed that OP-145 and I12K could not totally permeabilize the cell membrane at the time point, where the determined lethal concentration of the peptides was reached. In fluorescent leakage studies with model membranes consisting of the major membrane lipid components of Gram-negative bacteria these two peptides induced negligible permeabilization. Also P148 did not induce full permeabilization even at the highest concentration used.

Both calorimetric studies on membrane mimetic systems and fluorescence microscopy on bacteria indicated that all three peptides induce a disordering of the membrane components due to formation of lipid domains. This will result in defects at their boundaries inducing membrane perturbation and membrane permeabilization.

ZUSAMMENFASSUNG

Die Zunahme Antibiotika resistenter pathogener Keime stellt ein globales Gesundheitsproblem dar. Daher ist es notwendig Therapeutika mit neuartigen Wirkungsmechanismen zu entwickeln. Antimikrobielle Peptide, die im angeborenen Immunsystem von vielen verschiedenen Spezies zu finden sind, stellen wertvolle Ausgangsstrukturen dar, die für die Entwicklung solcher Agenzien von Bedeutung sind. Sie töten bakterielle Erreger vor allem durch die Schädigung der Plasmamembran innerhalb von Minuten ab. Die Permeabilisierung von Plasmamembranen wird stark von der unterschiedlichen Lipidzusammensetzung der Bakterien- und Säugermembran beeinflusst. Die kationischen und amphipathischen Peptide zeigen eine hohe Aktivität gegen negativ geladene bakterielle Membranen im Gegensatz zu neutralen Säugermembranen.

Das Ziel dieser Masterarbeit war die antimikrobielle Aktivität von drei humanen Cathelicidin LL-37 abgeleiteten antimikrobiellen Peptiden mit der Membranpermeabilisierung in Gram-negativen Bakterienstämmen wie *Escherichia coli* ATCC 25922 und *Escherichia coli* K12 5K sowie von Modellmembranen, die die innere Membran Gram-negativer Bakterienzellen nachahmen, zu korrelieren. Die untersuchten Peptide OP-145, P148 und I12K mit einer Länge von 24 Aminosäuren nehmen eine α -helikale Sekundärstruktur an. Sie interagieren bevorzugt mit dem negativ geladenen Phosphatidylglycerol (PG), das zu einer Störung der Membran führt.

P148 ist das Peptid mit der höchsten Aktivität gegen beide *E. coli* Stämme. Es erreicht die letale Konzentration ($LC_{99,9}$) bereits nach 5 Minuten bei einer Konzentration von 0,8 μ M. Während OP-145 eine verminderte aber ähnliche Aktivität bezüglich der beiden Stämme zeigt, ist die letale Konzentration von I12K sehr unterschiedlich zwischen den beiden *E. coli* Stämmen. Echtzeitmessungen der Membranpermeabilisierung zeigen, dass OP-145 und I12K zum Zeitpunkt der vorher ermittelten letalen Konzentration die Zellmembran nicht vollständig

permeabilisieren können. In Fluoreszenz abhängigen Studien mit Modelmembranen, die aus den Hauptmembranlipiden von Gram-negativen Bakterien bestehen, induzieren diese zwei Peptide nur eine vernachlässigbare Permeabilisierung. Auch das Peptid P148 selbst konnte bei der höchsten verwendeten Konzentration keine vollständige Permeabilisierung der Membran induzieren.

Allerdings zeigten kalorimetrische Untersuchungen an Modelmembranen als auch die Fluoreszenzmikroskopie an Bakterien, dass alle drei Peptide eine Störung der Membran durch die Bildung von Lipiddomänen verursachen. Diese können dazu führen, dass Defekte an deren Grenzflächen zu erhöhter Permeabilität führen.

I. INTRODUCTION

1. The problem of antibiotic resistance

Antibiotics have been beneficial for treatment of bacterial infections since the introduction of the first agents in the 1940s. The discovery and development of new classes of antibiotics mainly during the 1960s present an array of treatment options, which now has become more and more limited. The problem of antibiotic resistant pathogens that has been a concern since the beginning of the antimicrobial era, has increased recently (Powers, 2004; Lohner, 2017). Beside the environmental and demographic changes a main role for the global occurrence of antimicrobial resistant Gram-negative and Gram-positive bacteria is the excessive and unsuitable use of antibiotics for the treatment and prevention of bacterial infections in human as well as in animal health care. Another problem is the infection control in hospitals facilitating the emergence of drug-resistant strains, which can pass their resistance genes to other bacteria. There are pathogens like some MRSA (methicillin-resistant *S. aureus*) which are also resistant to the more costly second-line antibiotics. Currently there are only few antibiotics against these pathogens in development or in clinical trials. Since the 1980s the number of new antibiotics decreased obviously and only two completely new classes have been introduced on the market, the others were antibiotics with similar structures as the existing ones (Lohner, 2017).

A report from the World Health Organization in 2014 referred to alarming levels in bacterial resistance in many parts of the world and antibiotics with novel mechanisms of action should urgently be developed (World Health Organization, 2014). It is necessary to find therapeutic agents with a different mode of action but the same characteristics as conventional antibiotics. Furthermore, they should have low toxicity and a broad spectrum of activity. Antimicrobial peptides (AMPs) are valuable template structures for the development of such compounds to combat infectious diseases (Lohner, 2001)

2. Antimicrobial peptides

Antimicrobial peptides are a class of small, mostly cationic and amphipathic peptides that are considered to be promising candidates to fight microbial infections, by killing the bacteria with high potency and speed (Lohner, 2001).

During the last decade research on antimicrobial peptides has markedly increased as reflected by the more than 2600 natural or synthetic peptides listed in the Antimicrobial Peptide Database (APD2, <http://aps.unmc.edu/AP>) (Wang et al., 2008). The synthetic peptides are gained either by modification of natural peptides or by *de novo* synthesis and optimized for efficacy, selectivity and applicability (Lohner, 2017). Several of these peptides have already been clinically tested against localized infections (Andrès, 2012).

Antimicrobial peptides comprising 10 to 50 amino acids with a positive net charge have various structures and biological activity profiles (Wang et al., 2008). These peptides show a broad spectrum of activity against bacterial, viral and fungal pathogens (Andrès, 2012). The main advantage of these molecules considering bacterial resistance is their mode of action. In contrast to conventional antibiotics the host defensive (antimicrobial) peptides show their effects on bacteria within minutes, faster than their growth-rate, which makes the development of resistance less likely (Boman, 2003; Fjell et al., 2011). Furthermore most of these peptides are an intrinsic part of many living organisms and one of the key components of the innate immune defense (Hancock, 2001).

Antimicrobial peptides have different mechanisms to kill bacteria which are well described in reviews (Lohner, 2017; Hancock and Sahl, 2006; Nguyen et al., 2011). Besides permeabilizing the cell membranes, which is the main target of AMPs, through the direct interaction AMPs also can interfere with a series of cellular processes and metabolic functions like inhibition of cell division, septum formation and cell wall

biosynthesis. For this, peptides translocate through the cell membrane and interact with intracellular targets like nucleic acids and proteins (Lohner and Blondelle, 2005).

AMPs can disrupt the lipid bilayers through peptide carpeting or pore formation. After the coverage of the membrane surface by AMPs as an initial step the peptides can act in a detergent-like manner (Shai, 2002; Bechinger and Lohner, 2006) or form “toroidal pores” (Matsuzaki et al., 1996; Ludtke et al., 1996), in which the peptides together with the lipid head groups line the insight of the water-filled pore. AMPs can also form “barrel-stave” transmembrane pores (Shai and Oren, 2001). It was also shown that higher peptide concentrations can lead to bilayer thinning (Chen et al., 2003). Furthermore AMPs can bind to specific lipids and induce lipid phase separation (Lohner et al., 1997) or micellization of lipid bilayers at very high peptide concentrations (Bechinger and Lohner, 2006). These peptides can also lead to membrane dysfunctions by forming lipid-peptide domains or non-lamellar phases (Lohner and Blondelle, 2005). To identify the mechanisms described liposomes that mimic mammalian and bacterial cell membranes are used.

3. Biological cell membranes

The cell membrane consisting of a phospholipid bilayer with integrated proteins is a semi-permeable barrier between the cytoplasm (interior) and the periplasm (outside) of a cell. Besides the important protective function it is also involved in many other biological processes like synthesis and secretion of proteins, transport of ions and molecules across the membrane, regulating the cell-growth and recognition of cells or signal transduction through transmembrane receptors. Depending on species biological membranes could include also glycolipids, sphingolipids or sterols and can be described by the fluid mosaic model (Singer and Nicolson, 1972). The lipid composition of the membranes does not

only differ between two species, but it also varies between different membranes of a single cell.

The plasma membrane of erythrocytes, which is a representative of mammalian cells, mainly consists of about 60 % of the four major phospholipids phosphatidylcholine (PC), phosphatidylethanolamine (PE) phosphatidylserine (PS), and sphingomyelin (SM) and 25 % of cholesterol. As shown in Figure 1, there is an asymmetric distribution of phospholipids between the outer and inner lipid leaflet of the bilayer exposing PC and SM predominantly to the extracellular side and therefore neutral-charged at physiological pH (Rothman and Lenard, 1977). This asymmetry is maintained by an ATP-dependent translocase.

Plasma membranes of bacteria however are negatively charged due to the presence of anionic phospholipids. Whereas Gram-negative bacteria have a larger amount of PE and to a lesser extent negatively charged phosphatidylglycerol (PG) and cardiolipin (CL), in Gram-positive bacteria the negatively charged PG is the major component of the cytoplasmic membrane (Figure 1). The lipids of Gram-negative bacteria are mostly composed of C16:0, C16:1 and C18:1 fatty acids (Latal et al., 1997; Malanovic and Lohner, 2016).

By consideration of the phospholipid components of the bacterial membrane, it can be said that the plasma membrane of Gram-positive bacteria is more negatively charged than the membrane of Gram-negative strains. Like it is shown in Figure 1, microbial plasma membranes are in contrast to higher living organisms surrounded by a cell wall of a tight and flexible layer composed of lipopolysaccharides (in Gram-negative bacteria) and peptidoglycan (in Gram-positive strains) (Malanovic and Lohner, 2016).

Through the different physicochemical properties of these lipids in biological membranes, the peptides can distinguish between bacterial and mammalian cell membranes. The

cationic AMPs interact preferentially with the negatively charged bacterial membranes and therefore have a lower affinity towards the host cells (Lohner, 2009). Our focus in this study was on the permeabilization of Gram-negative bacteria and respective model membranes by antimicrobial peptides.

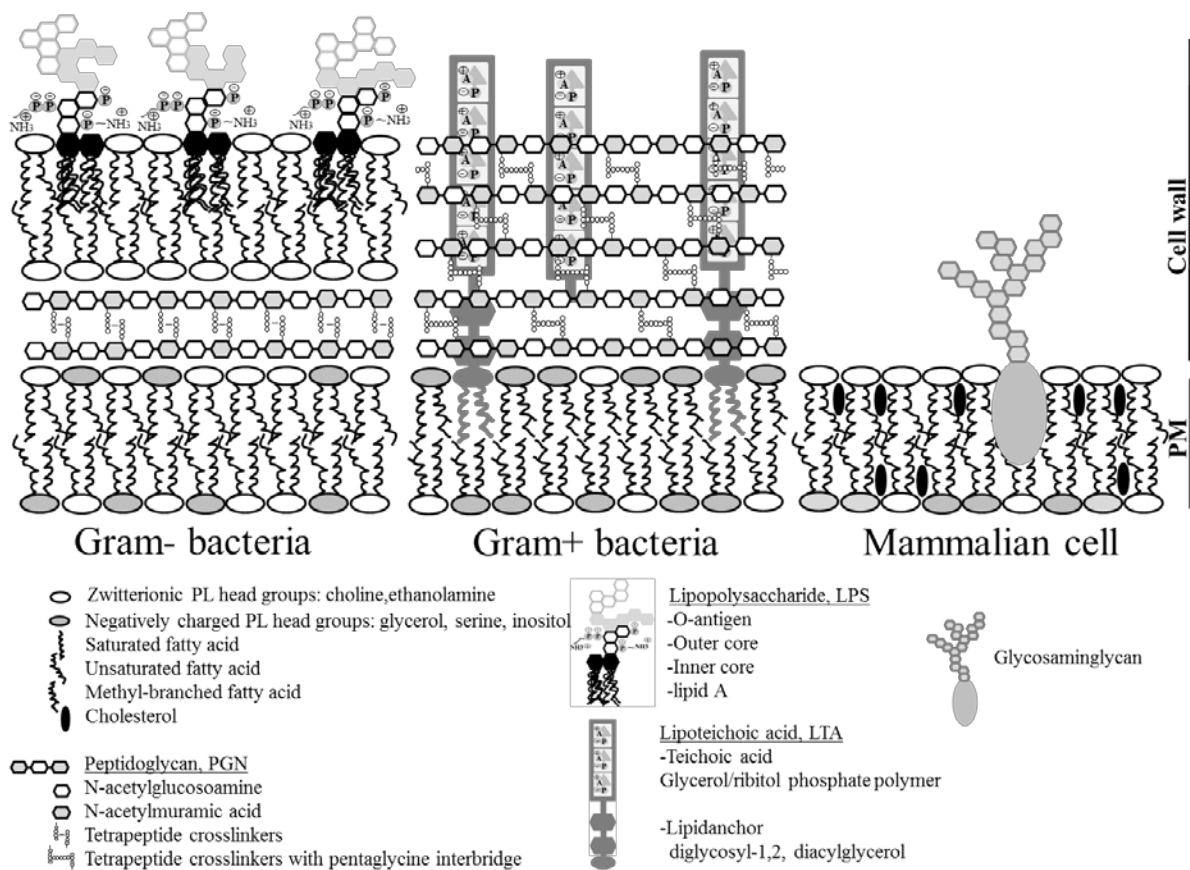


Figure 1: Cell envelopes of Gram-negative & Gram-positive bacteria and mammalian cells. Modified figure from (Malanovic and Lohner, 2016).

4. Phospholipids

Phospholipids are amphipathic molecules consisting of a hydrophilic (polar) head group and a lipophilic tail which is hydrophobic. The predominant phospholipids in Gram-negative bacterial species are PE, PG and CL, which were used in model membrane experiments. With these lipids liposomes were formed that mimic bacterial cell membranes of Gram-negative strains.

PE is a fully hydrated zwitterionic lipid containing less water than for example PC leading to a truncated cone shape of the molecule. PG however, a lipid with a negative net charge, has a cylindrical shape. CL is also a negatively charged phospholipid having four acyl chains and two phosphate groups. Structures of the phospholipids used in this study are shown in Figure 2. For PG and PE two different types of phospholipids were used depending on the experiments, saturated and unsaturated ones.

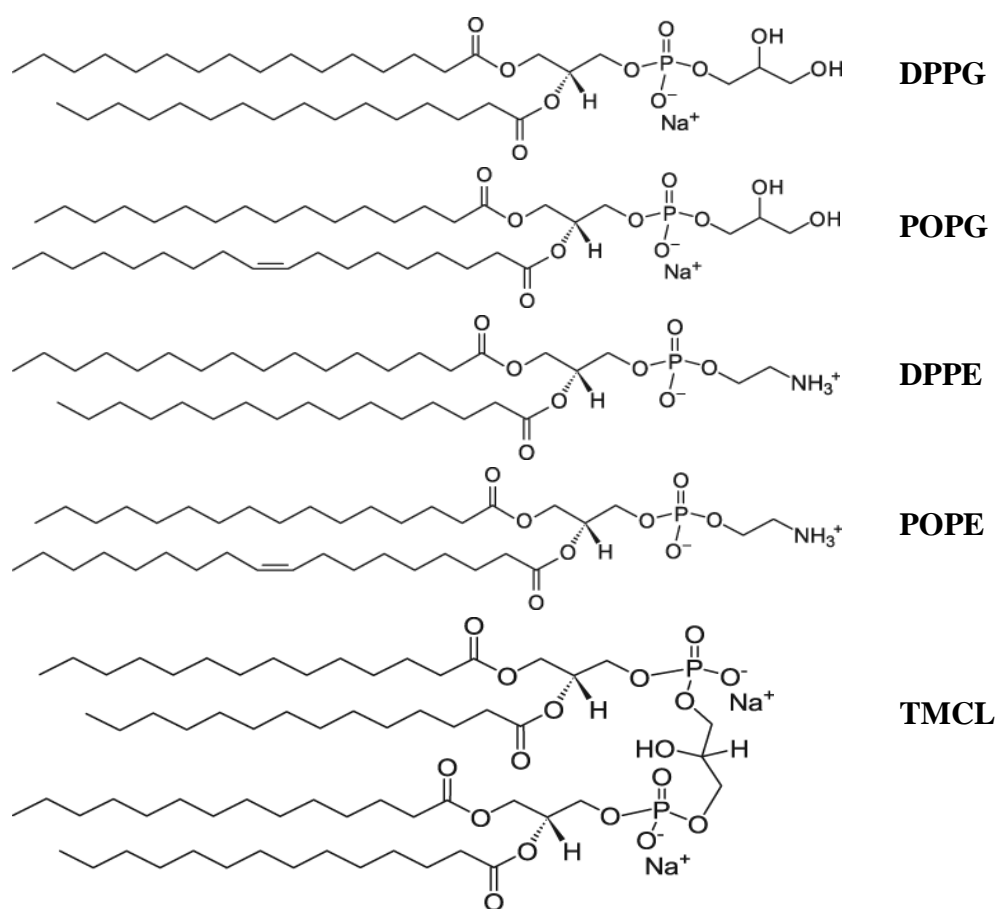


Figure 2: Structures of the phospholipids used in this study, taken from Avanti Polar Lipids

5. Human cathelicidin LL-37, an antimicrobial peptide

Human LL-37, released from the precursor hCAP18, is one of the best studied cationic and amphipathic antimicrobial peptides, which belongs to the cathelicidin peptide family. Besides its activity against a wide spectrum of bacteria, fungi and viruses the peptide also plays an important role in innate host defense by regulating the inflammatory response and chemo-attracting cells of the adaptive immune system to wound or infection sites and promoting re-epithelialization and wound closure (Durr et al., 2006; Nell et al., 2006). LL-37 and its precursor hCAP18 are expressed in many cell types and body fluids including epithelial cells of the skin, the gastrointestinal tract and the respiratory tract and in leukocytes such as monocytes, neutrophils, T cells, NK cells, and B cells.

Figure 3 shows the structure of LL-37 composed of 37 amino acids with the sequence LLGDFFRKSKEKIGKEFKRIVQRIKDFLRNLPRTES at physiological conditions. The peptide has a net charge of +6 at physiological pH and adopts an amphipathic α -helical secondary structure (Burton and Steel, 2009), with hydrophobic residues on one side of the helix and hydrophilic residues on the other side of the helical structure (Figure 3A).

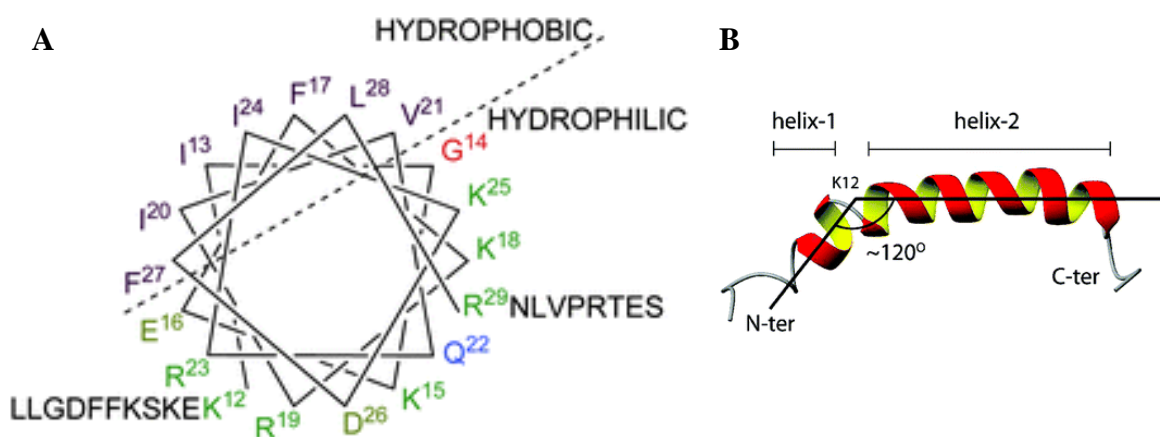


Figure 3: Structure of the human antimicrobial peptide LL-37. (A) Shows the helical wheel diagram of the region 12-29 as an amphipathic helix. N- (residues 1-11) and C- (residues 30-37) termini residues are unstructured (Burton und Steel 2009). (B) NMR structure of LL-37 showing the angle between the two helical domains and the break point centered at K12 (Porcelli et al., 2008).

Besides to other natural antimicrobial peptides, which typically assume a secondary structure only upon membrane binding, LL-37 can form α -helical aggregates (secondary structures) in aqueous solution depending on its concentration leading to a resistance against proteolytic degradation in solution and when bound to membranes (Oren et al., 1999; Durr et al., 2006).

Through its amphipathicity LL-37 can interact electrostatically with anionic bacterial membranes. Beginning with depolarization and destabilization of the cell membrane the peptide can penetrate the membrane, form transmembrane pores and subsequently cause lysis of bacteria. Cholesterol including cellular membranes like those in mammalian cells however protects from the pore-forming effects of LL-37 at low peptide concentrations (Kahlenberg and Kaplan, 2013).

6. Antimicrobial peptides used in this thesis: OP-145, P148 and I12K

To improve the activity of LL-37 against bacterial strains modifications in the sequence of the peptide have been introduced. In a study (Nell et al. 2006) the LL-37 sequence was scanned with a window size of 22 to 25mers identifying a 24mer (amino acid sequence 13-36, helix 2 in Figure 3) as the most promising segment in terms of antimicrobial activity which is similar to LL-37.

After some modifications in the sequence and amino acid replacements at the C-terminus to favor the formation of an ideal amphipathic helix, the peptide OP-145 (previously termed P60.4Ac) with the sequence acetyl-IGKEFKRIVERIKRFLRELVRPLR-amide (Figure 4) was derived (Nell et al., 2006). To improve the stability of this peptide against proteolytic degradation the N-terminus was blocked by acetylation and the C-terminus by amidation (Nell et al., 2006). In addition, this peptide is characterized by a lateral amphipathicity having polar and charged residues along one side of the helix and

hydrophobic amino acids on the other. OP-145 was tested against Gram-positive strains, showing high efficiency against MRSA (methicillin-resistant *S. aureus*) and being able to eliminate biofilm-associated bacteria (Nell et al., 2006; Haisma et al., 2014). There were no toxic effects detected on human epidermal models (Haisma et al., 2014). Furthermore the activity of the peptide against membranes was tested on bacterial and mammalian membrane mimics (Malanovic et al., 2015). Further studies showed that the peptide can prevent *Staphylococcus aureus* biomaterial-associated infections (BAI) using a polymer-lipid coating containing OP-145 resulting in the inhibition of biofilm formation and protection against infections (Breij et al., 2016).

From OP-145 new AMPs with the same chain length were developed including P148 with the sequence acetyl-LKRVWKR VFKLLKRYWRQLKKPVR-amide and I12K with the sequence acetyl-IGKEFKRIVERKKRFLRELVRPLR-amide. The structures of all three peptides are shown in Figure 4.

In comparison to OP-145, the negative charges (E10 and E18) were eliminated in P148 resulting in a peptide with a higher net positive charge. In addition the peptide is characterized by a higher total hydrophobicity. This is important for the initial binding of the peptide to anionic membrane phospholipids and it would lead to a stronger membrane partitioning, presumably resulting in stronger membrane disruption. Furthermore, this peptide has 2 tryptophan residues which seem to be important for the insertion into the interfacial region of the phospholipid bilayer especially negatively charged lipid bilayers and hence their disruption (Schibli et al., 2002).

If we look at the structure of the antimicrobial peptide I12K, we see that there is only a difference in one amino acid comparing to OP-145. At sequence number 12 the nonpolar amino acid isoleucine was exchanged by the basic polar amino acid lysine which leads to a break of the hydrophobic face inducing a kink in the α -helix (Figure 4).

In this thesis the activity of the peptides OP-145, P148 and I12K concerning membrane permeabilization was tested with two *E. coli* strains, as representatives of Gram-negative bacteria, and with model membranes mimicking Gram-negative plasma membranes.

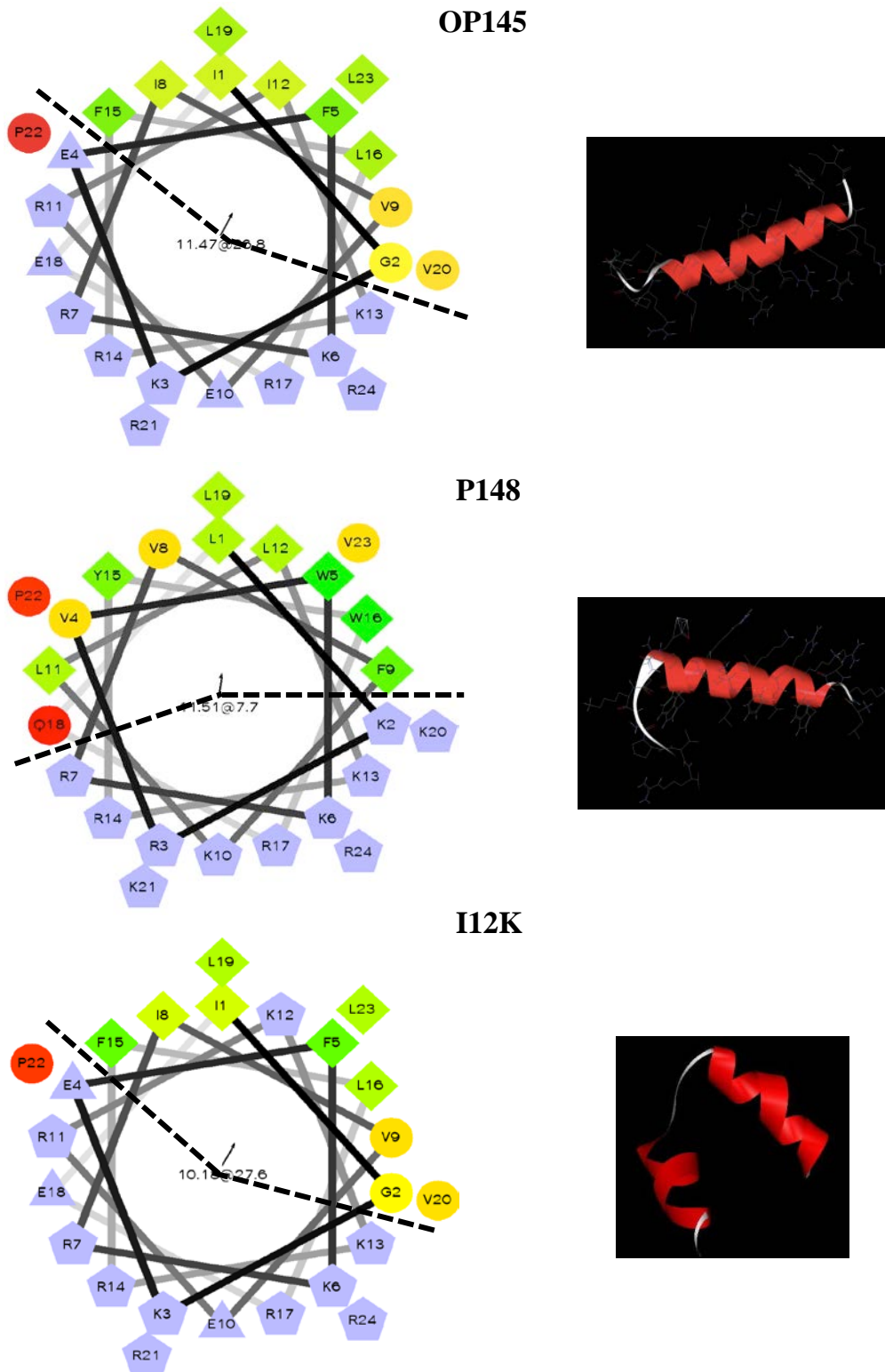


Figure 4: Presentation of the AMPs OP-145, P148 and I12K which were used in this thesis in a helical wheel diagram (left panel) and as α -helices by Mobylye@RPBS (right panel).

II. MATERIALS AND METHODS

1. Peptides

The peptides with their corresponding sequences used in this study are listed in Table 1.

Table 1: Antimicrobial peptides and their sequences used in this study.

Peptide	N-terminus	Sequence N-C	C-terminus
OP-145	acetyl	IGKEFKRIVERIKRFLRELVRPLR	amide
P148	acetyl	LKRVWKR VFKLLKRYWRQLKKPVR	amide
I12K	acetyl	IGKEFKRIVERKKRFLRELVRPLR	amide

They were synthesized and obtained from our collaborator Jan W. Drijfhout from the Department of Immunohematology and Blood Transfusion, Leiden University Medical Center, Leiden, The Netherlands. The peptides were stored at -20 °C until use, then dissolved in 0.1 % acetic acid pH 3.3 to a stock of 10 mg/ml. Aliquots were also stored at -20 °C. Concentration of P148 was determined by measurement of UV-absorbance of tryptophan at 280 nm with PEQLAB Nano Drop ND-1000 Spectrophotometer, Erlangen, Germany. For other two peptides which do not bear tryptophan residues theoretical estimation of the concentration which encompasses all counter ions in the peptide (Na⁺ and trifluoroacetate, TFA) including 10% water was calculated. Such calculation gives nearly exact concentration as it was verified by 280 nm absorbance for P148.

2. Lipids

All phospholipids (>99% purity) were obtained from Avanti Polar Lipids (Alabaster, AL) and stored at -20°C before usage. The used lipids are DPPG (1,2-dipalmitoyl-sn-glycero-3-[phospho-rac-(1-glycerol)], Sodium Salt, MW = 744.96 g/mol), DPPE (1,2-dipalmitoyl-sn-glycero-3-phosphoethanolamine, MW = 691.97 g/mol), TMCL (1,1',2,2'-tetramyristoyl cardiolipin, Sodium Salt, MW = 1285.62 g/mol), POPG (1-palmitoyl-2-oleoyl-sn-glycero-3-[phospho-rac-(1-glycerol)], Sodium Salt, MW = 770.99 g/mol),

POPE (1-palmitoyl-2-oleoyl-sn-glycero-3-phosphoethanolamine, MW = 718.01 g/mol), *E. coli* Polar Lipid Extract (PE 67%, PG 23.2%, CL 9.8%) and *E. coli* Total Lipid Extract (PE 57.5%, PG 15.1%, CL 9.8%, unknown 17.6%).

3. Preparation of liposomes

To prepare lipid films for differential scanning calorimetry (DSC) 10 mg/ml stock solution of every single lipid in an appropriate solvent have been made first. DPPG, DPPE, POPG and POPE were dissolved in chloroform/methanol 9:1 v/v, TMCL in chloroform and the *E. coli* lipids in chloroform/methanol 2:1 v/v. Further, lipid mixtures like DPPG/DPPE (25/75), DPPG/DPPE/TMCL (20/60/10), POPG/POPE (25/75), POPG/POPE/TMCL (20/60/10) with a total amount of 1 mg were made by mixing the appropriate amount of phospholipids needed (Table 2) calculated with formula 1.

$$\text{Formula 1. } mA [mg] = \frac{mol\% * mA}{mol\% * mA + mol\% * mB}$$

mA stands for the molecular weight of one lipid and mB the molecular weight of the other lipid, $mol\%$ is the molecular percentage of one lipid component in the lipid mixture.

The lipid mixtures were evaporated under a stream of nitrogen for 30 minutes at 35°C and afterwards dried in vacuum overnight. Lipid films were stored at 4°C until use.

Table 2: Amount of phospholipids for preparing lipid films with a total lipid amount of 1 mg.

Lipid film	MW [g/mol]	DPPG [mg]	DPPE [mg]	TMCL [mg]	POPG [mg]	POPE [mg]
DPPG/DPPE (25/75)	705.2	0.264	0.736			
DPPG/DPPE/TMCL (20/60/10)	769.7	0.215	0.599	0.186		
POPG/POPE (25/75)	731.3				0.263	0.736
POPG/POPE/TMCL (20/60/10)	792.9			0.180	0.216	0.604

For the formation of lipid vesicles 1 ml sodium phosphate buffer (20 mM NaPi, 130 mM NaCl, pH 7.4) was added to the lipid films. In the case of peptide containing vesicles, peptides were added to lipid films with a molar ratio lipid/peptide 25:1 and 100:1 for DPPG/DPPE and DPPG/DPPE/TMCL at the final volume of 1 ml (total concentration of 1 mg/ml). For POPG/POPE and POPG/POPE/TMCL the peptides were added with the molar ratio lipid/peptide 25:1. Formation of lipid vesicles was achieved by vortexing at the time points 0', 5', 10', 20', 30' and 60' for 1 minute. All probes were incubated at a temperature above the phase transition of the respective phospholipids, in this case in a sand bath at 65 °C for one hour. The prepared liposomes were stored at room temperature until using them for Differential Scanning Calorimetry (DSC).

For leakage measurements liposomes with concentration of 20 mg/ml in fluorophore-buffer (10 mM Hepes, 68 mM NaCl, 12.5 mM ANTS, 45 mM DPX, pH 7.4) were used. Large unilamellar vesicles (LUVs) of ca. 100 nm were obtained by extrusion of the hydrated liposomes applying 20 cycles through a polycarbonate filter (Millipore-IsoporeTM) of 0.1 µm pore size (Zweytick et al., 2011). ANTS (8-aminonaphthalene-1,3,6-trisulfonic acid, disodium salt) and DPX (p-xylene-bis-pyridinium bromide) were purchased from Molecular Probes (Eugene, OR). Size of the vesicles was measured using the Zeta sizer (Zetasizer NANO, Malvern Instruments, Herrenberg, Germany).

4. Differential Scanning Calorimetry (DSC)

DSC measurements were performed using a Microcal VP-DSC high-sensitivity differential scanning calorimeter (Microcal, Northampton, MA). Scans of 1 mg/ml lipid concentration were recorded at a constant rate of 30 °C/h and data were analyzed using Microcal's Origin software (Malanovic et al., 2015).

DPPG/DPPE and DPPG/DPPE/TMCL – liposomes were measured between 10-70 °C whereas POPG/POPE and POPG/POPE/TMCL – liposomes were measured from 1-75 °C. Calorimetric enthalpies were calculated by integration of the peak areas after baseline correction and normalization to the mass of phospholipid. The phase transition temperature was defined as the temperature at the peak maximum.

5. Phosphate determination

To determine the phosphate content of the prepared unilamellar liposomes (20 mg/ml) a standard protocol described by (Broekhuysen, 1968) was used. Briefly, samples were warmed up for a minute at 180 °C before incubation with 0.4 ml acid mixture ($\text{H}_2\text{SO}_4:\text{HClO}_4 = 9:1$) for further 30 minutes. ANSA-molybdate mixture was added to the cooled samples and incubated for 20 min at 90°C. The ANSA reagent contained 10.5 mM α ANSA (1-amino-2-hydroxy-naphthalin-4-sulfonic acid), 0.7 mM $\text{Na}_2\text{S}_2\text{O}_5$ and 40 mM Na_2SO_3 , the used NH_4 -Heptamolybdate had 0.26 % (w/v).

Extinction of the cooled samples was measured at 830 nm using a Spectronic® 20 genesysTM photometer (Spectronic Instruments, USA) which is directly proportional to the phosphorus content in the samples. Phospholipid concentration was determined from the calibration curve, which was prepared from the amount of 1-14 μg phosphorus using 3.2 mM KH_2PO_4 as a P-standard solution.

KH_2PO_4 and α ANSA were purchased from E. Merck, Darmstadt, Germany; $\text{Na}_2\text{S}_2\text{O}_5$, Na_2SO_3 and H_2SO_4 (96 % v/v) from Carl Roth, Karlsruhe, Germany; ammonium molybdate tetra-hydrate and HClO_4 (67-72 % v/v) from Sigma-Aldrich, Steinheim, Germany.

6. Fluorescence spectroscopy and leakage assay

Leakage of the aqueous content of the 8-aminonaphthalene-1,3,6-trisulfonic acid/p-xylene-bis-pyridinium bromide (ANTS/DPX)-loaded liposomes (large unilamellar vesicles) composed of POPG/POPE, POPG/POPE/TMCL and *E. coli* lipid extracts (polar/total) upon incubation with peptide was determined as described (Zweytick et al., 2011). Briefly, 20 mg/ml ANTS/DPX loaded lipid vesicles of defined size were separated from free fluorescent dye by exclusion chromatography using a column filled with SephadexTM G-75 (Amersham Biosciences) fine gel swollen in an iso-osmotic buffer (10 mM HEPES, 140 mM NaCl, pH 7.4). The phospholipid concentration was determined by phosphate analysis as described above. Fluorescence emission from the ANTS/DPX loaded lipid vesicles was obtained at 37 °C (physiological temperature) at an excitation wavelength of 360 nm and an emission wavelength of 530 nm. Slit width for excitation and emission monochromators was 10 nm. The fluorescence measurements were performed in quartz cuvettes in 2 ml of the iso-osmotic buffer at the referred temperature. Lipids were added with a final concentration of 50 µM. Fluorescence emission was recorded as a function of time before and after the addition of incremental amounts of peptide ranging from 0.13 up to 16 µM, corresponding to peptide-to-lipid molar ratios from 1:400 to 1:3.1. The measurements were performed on a VARIAN Cary Eclipse fluorescence spectrophotometer combined with Cary Eclipse Software (Scan). Percentage of leakage was calculated from the fraction of the leakage (I_F) according to the following

$$\text{formula: } I_F = \frac{(F - F_0)}{(F_{max} - F_0)}$$

where F is the measured fluorescence, F_0 is the initial fluorescence without peptide, and F_{max} is the fluorescence corresponding to 100% leakage gained by addition of 20 µl 10% Triton X-100 (Zweytick et al., 2011; Malanovic et al., 2015).

7. Bacterial strains and growing conditions

Two different bacterial strains have been used,

Escherichia coli K12 5K (tre, thi, rpsL+, kdsR, kdsM+, lac) (Koraimann and Högenauer, 1989), obtained from Gertrude Zisser, Institute of Molecular Biosciences, University of Graz and

Escherichia coli ATCC 25922 (Thermo Scientific, Lenexa, KS 66215, USA). The cells were rehydrated according to the description in the product shield.

Overnight cultures have been made from single colonies in Mueller Hinton Broth (MHB, Carl Roth, Karlsruhe, Germany) by incubating the cells at 37 °C and 200 rpm.

Mueller Hinton Broth contains beef infusion (2.0 g/l), casein peptone (acidic hydrolysate) (17.5 g/l) and corn starch 1.5 g/l. The pH value is 7.4 ± 0.2 . Main culture has been made with an inoculum of 0.05 for *E. coli* ATCC 25922 and 0.1 for *E. coli* K12 5K. The cultures were grown until the mid-logarithmic phase which was reached after 3 hours by *E. coli* K12 5K and 3.5-4 hours by *E. coli* ATCC 25922. The bacteria reached the stationary phase after about 10 hours.

8. Antimicrobial activity

E. coli ATCC 25922 and *E. coli* K12 5K were cultured to mid-logarithmic phase in MHB at 37 °C under shaking conditions (200 rpm) and washed once with NaPi-buffer. Approximately 1×10^6 CFU/ml in NaPi (calculated from the absorbance of the suspension at 600 nm) were incubated with OP-145 (final concentrations: 0 - 6.4 μ M for both strains), P148 (final concentrations: 0 - 1.6 μ M for both strains), I12K (final concentrations: 0 - 25.6 μ M for *E. coli* ATCC 25922 and 0 - 6.4 μ M for *E. coli* K12 5K) for 2 h at 37°C under shaking conditions (300rpm). Thereafter, the number of viable bacteria was determined by plating 10-fold serial dilutions of 100 μ l sample on diagnostic sensitivity

agar, Müller Hinton Agar (MHB+2 w % Agar). The same experiment was also done in a time dependent way, where the antimicrobial activity was determined after 5, 10, 20, 30, 60 and 120 minutes at the above described peptide concentrations. Antimicrobial activity is expressed as the 99.9 % lethal concentration (LC_{99.9}), i.e., the lowest peptide concentration that killed ≥ 99.9 % of bacteria (Malanovic et al., 2015).

9. Membrane permeabilization using living bacteria by flow cytometry

Both *E. coli* strains were cultured to mid-logarithmic phase at 37 °C under vigorous shaking and then washed once with NaPi-buffer (5 min 5000 g). This bacterial suspension was diluted in NaPi to 1×10^6 CFU/ml, as calculated from the absorbance of the suspension at 600 nm and stored on ice. 600-1200 μ l of the cell suspension were incubated five minutes at room temperature with propidium iodide (PI, 1 μ g/ml final concentration in sample) in the dark. Afterwards the sample was transferred in polystyrene-tubes and PI fluorescence was measured with BD LSR FortessaTM in real-time using the BD FACSDiva Software (excitation 488 nm; emission detection at 695/40 nm, PerCP-Cy5.5 channel). Selective gating was used to discriminate between PI-positive and -negative cell populations. Voltage of the PerCP-Cy5.5 channel was adjusted to yield relative fluorescence values >700 (PerCP-Cy5.5 peak area) for PI-positive cells. The measuring rate was at about 300-400 events per second. After approximately 30 seconds defined peptide solutions were added to the labeled bacterial cells, mixed and fluorescence of PI was followed for 5 to 20 minutes depending on peptide, concentrations and times are listed in Table 3.

Table 3: Concentration of peptides and measuring time depending on bacterial strains for the FACS measurements.

strain	peptides	concentration [μM]	time [min]	strain	peptides	concentration [μM]	time [min]
<i>E. coli</i>	OP-145	1.6 – 12.8 μM	20	<i>E. coli</i>	OP-145	1.6 – 6.4 μM	20
ATCC	P148	0.4 – 1.6 μM	5/10	K12	P148	0.1 – 1.6 μM	5
25922	I12K	6.4 – 25.6 μM	20	5K	I12K	1.6 – 6.4 μM	20

The percentage of PI-positive cells was calculated at different time intervals after the extraction of the fcs-files from the BD FACSDiva Software into csv documents (using FCSExtract Utility, version 1.02) and further analyzed with Microsoft Excel. In order to calculate the fraction of PI-positive cells the number of events with >700 PerCP-Cy5.5 peak area (defined as PI-positive cells) were divided by the total number of events of a given time interval (i.e. 60 seconds).

10. Fluorescence Microscopy

E. coli strains were cultured to mid-logarithmic phase at 37 °C and 200 rpm, washed once with NaPi-buffer (5 min 5000 g). This bacterial suspension was diluted to 5×10^7 CFU in 200 μl NaPi, as calculated from the absorbance of the suspension at 600 nm. The cells were incubated with peptide concentrations 2-3 times lower than their $\text{LC}_{99,9}$ for 20 minutes at 37 °C and 300 rpm before they have been stained with 10 $\mu\text{g/ml}$ Nile Red (Sigma Aldrich, Steinheim, Germany), a fluorescent membrane dye. Nile Red stock solution of 1 mg/ml was prepared in methanol (Carl Roth, Karlsruhe, Germany). One minute later the cells get centrifuged and 1 μl of the pellet was mounted on a microscope slide with agar (2 w %) and covered with a coverslip of 0.17 μm thickness (Menzel, Inc.). Therefore 50 ml of 2 % agar (Sigma, Inc.) was melted at 600 W for 5 minutes in a microwave oven and 3 ml of the agar solution was pipetted on a standard microscope slide and hardened for 15 minutes at RT.

Microscopy was performed using a Leica SP5 confocal microscope (Leica Microsystems, Inc.) with spectral detection and a Leica HCX PL APO CS 63x NA 1.4 oil immersion objective. Nile Red was excited at 561 nm and fluorescence emission was detected between 570-750 nm. The 488 nm laser line was additionally activated for simultaneous acquisition of fluorescence and transmission data. Images were recorded using 47x47 nm sampling (x/y).

III. RESULTS

1. Antimicrobial activity

Antimicrobial activity of the peptides OP-145, P148 and I12K was tested by a standard killing assay (Malanovic et al., 2015). Briefly, after the cells reached the mid-log phase they were incubated with peptide for two hours and afterwards plated on a diagnostic sensitivity agar. Next day the colonies were counted and the colony forming units (CFU) per ml determined. Lethality is defined as the concentration, where 99.9 % of the bacteria were killed. Although the peptides show different cytotoxic activities against the two strains, in general they were highly effective against *E. coli*.

First step was testing the killing concentrations of the peptides (0.8 – 51.2 μM) after 2 hours incubation with the cells at 37 °C (data not shown). Depending on the results several concentrations for each AMP were chosen and the killing was tested over time (Figure 5). *E. coli* ATCC 25922 was incubated with 1.6 - 12.8 μM OP-145, 0.4 - 1.6 μM P148 and 6.4 - 25.6 μM I12K, whereas *E. coli* K12 5K was incubated with 1.6 - 6.4 μM OP-145 and I12K and 0.4 - 1.6 μM P148.

OP-145 was lethal against *E. coli* ATCC 25922 within 20 minutes at a concentration of 3.2 μM and against *E. coli* K12 5K within 10-20 minutes at a peptide concentration of 1.6-3.2 μM . Both strains were killed within 5 minutes with 6.4 μM OP-145. P148 is the peptide which showed the highest cytotoxic activity killing the bacteria within 5 minutes at a concentration of 0.8 μM and after 2 hours incubation they were also dead at 0.4 μM P148. I12K shows different activities on the two *E. coli* strains. For the *E. coli* K12 5K strain the lethal effect was reached in 20-30 minutes at 3.2 μM peptide concentration. For the *E. coli* ATCC 25922 a higher concentration of I12K is needed, the lethal concentration is between 12.8-25.6 μM . At 25.6 μM it takes about 5 minutes to kill all bacteria and at 12.8 μM 99 % death was reached after 5 minutes and it took up to 2 hours to reach $\text{LC}_{99.9}$.

The following experiments were mainly based on these peptide concentrations.

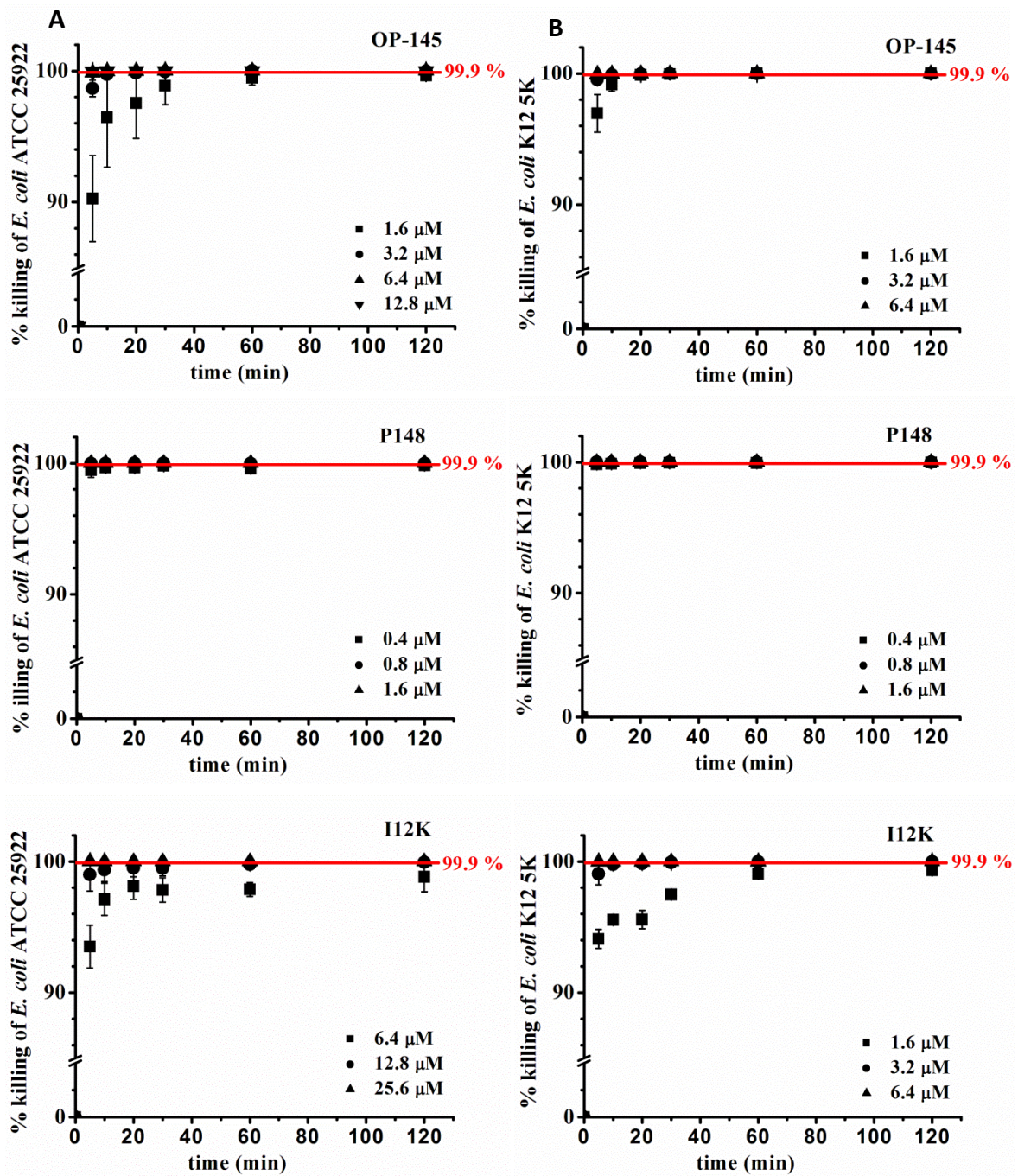


Figure 5: Killing of *E. coli* ATCC 25922 (A) and *E. coli* K12 5K (B) upon incubation with the peptides OP-145, P148 and I12K. All samples were incubated for 2 hours and the CFU was counted by plating after 5, 10, 20, 30, 60 and 120 minutes. The red line shows the point where $\geq 99.9\%$ of the bacteria were killed. The *E. coli* ATCC 25922 strain was incubated with 1.6 - 12.8 μM OP-145, 0.4 - 1.6 μM P148 and 6.4 - 25.6 μM I12K whereas the other strain was incubated with 1.6 - 6.4 μM OP-145 and I12K and 0.4 - 1.6 μM P148.

2. Membrane permeabilization

2.1 Permeabilization of living *E. coli* cells

The ability of the peptides to permeabilize living bacterial cells was tested by a propidium iodide (PI) cell viability assay. PI is a non-permeable fluorescent dye which cannot penetrate intact cell membranes. By damage of the cell membranes like in case of antimicrobial peptides PI penetrates into the cytosol resulting in a change of PI fluorescence which can be followed in real-time. PI-unstained *E. coli* cells, PI-stained *E. coli* cells and PI positive *E. coli*'s have a different distribution (Figure 6). The first two graphs (A, B top in Figure 6) show us also, if the staining of the bacterial cells was successful or not. The last graph (C top) in Figure 6 shows us how the distribution looks like when more than 95 % of the cells were PI-positive. In the bottom panel PI-positive cells are marked in a red color and the living cells are black.

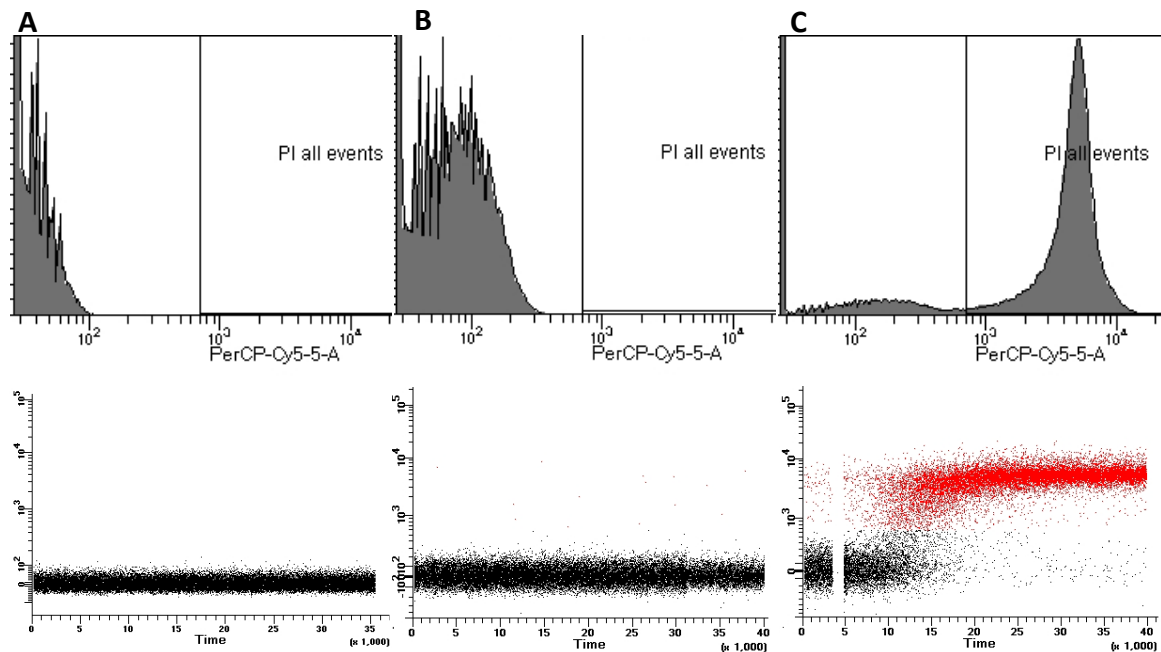


Figure 6: Distribution of *E. coli* cells during the FACS measurement. 1×10^6 CFU/ml were incubated 5 minutes (A) without PI, (B) with $1 \mu\text{g/ml}$ PI and (C) with $1 \mu\text{g/ml}$ PI and $0.8 \mu\text{M}$ P148, which was added approximately after 30 seconds. PI-positive cells are seen in red and the other cells in black. The time point 6 in the scale represents one minute.

After the staining control was done the cells were measured during incubation with different peptide concentrations. OP-145 and I12K were measured for 20 minutes and P148 for 5 minutes.

In the left panel of Figure 7 membrane permeabilization in *E. coli* ATCC 25922 of each peptide's killing concentration measured by propidium iodide influx is shown and in the right panel the percentage of PI-positive cells during time of all measured concentrations.

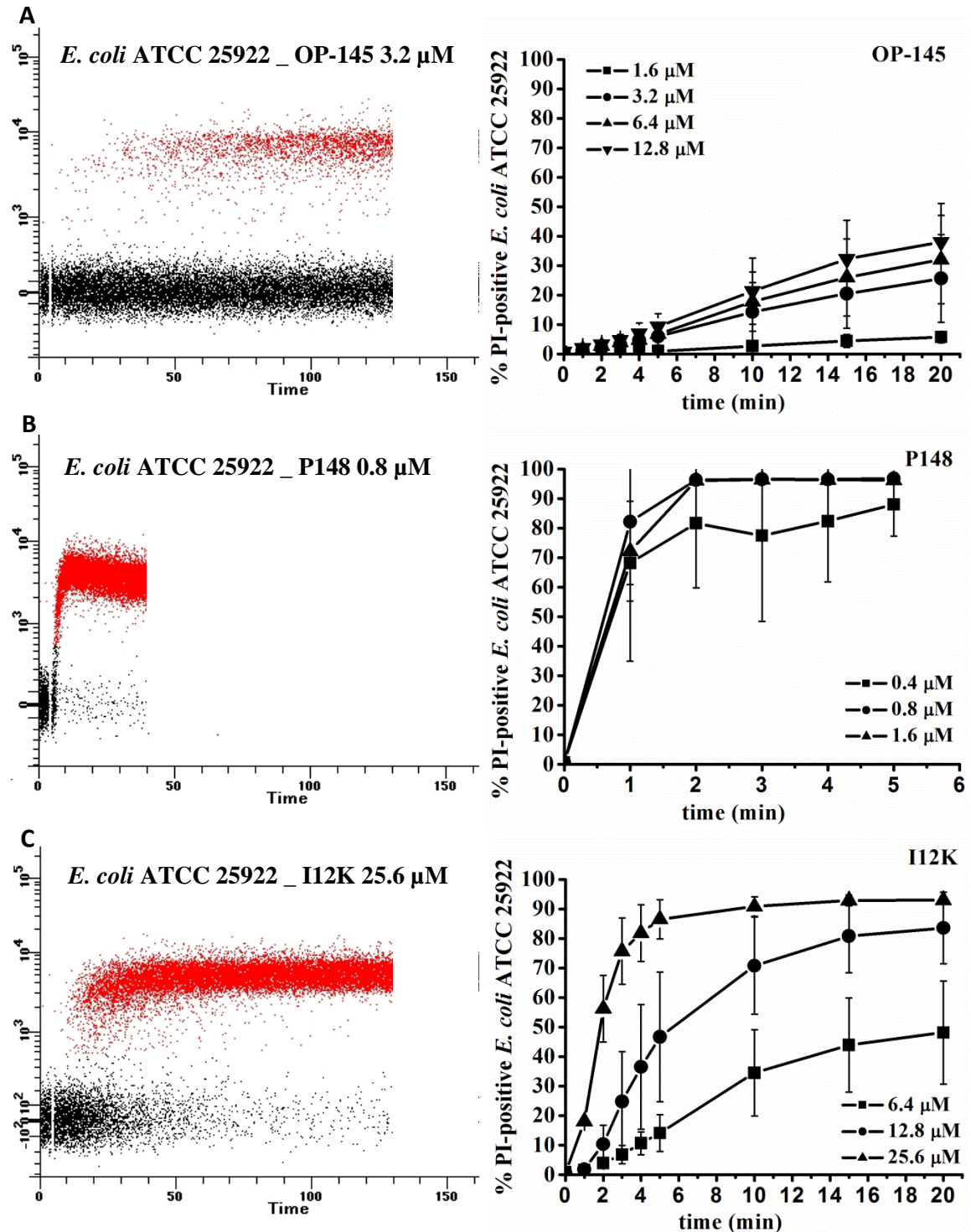


Figure 7: Membrane permeabilization in *E. coli* ATCC 25922 by the peptides (A) OP-145, (B) P148 and (C) I12K. Propidium iodide influx (left panel) and quantification of PI-positive *E. coli* (right panel). The peptides were added after 30 seconds and PI-fluorescence was measured during 20 minutes for OP-145 and I12K, and 5 minutes for P148. The percentage of PI-positive *E. coli* was calculated at different time intervals after addition of 1.6 - 12.8 μ M OP-145, 0.4 - 1.6 μ M P148 and 6.4 - 25.6 μ M I12K. Results are means of three independent experiments. Time point 6 in the scales of the left panel represents one minute.

OP-145 shows 32 % permeabilization of the *E. coli* ATCC 25922 cell-membranes at a concentration of 6.4 μM . At the killing concentration of 3.2 μM only 26 % of the cells were PI-positive (Figure 7A, right panel). The highest activity was induced by the peptide P148, which permeabilized the cell-membranes within 5 minutes at concentration of 0.8 μM (Figure 7B, right panel). About 90 % of the measured *E. coli* cells were PI-positive at the concentration of 25.6 μM I12K (Figure 7C, right panel).

The red color in the left panels in Figure 7 and 8 marked the PI-positive cells, whereas the other cells are shown in black. The time point of peptide addition is approximately after 30 seconds. Figures shown are representatives from several measurements.

The same measurements were also performed with the *E. coli* K12 5K strain only with different peptide concentrations. The left panel of Figure 8 shows the membrane permeabilization in *E. coli* measured through the propidium iodide influx at the defined killing concentrations of each peptide. In the right panel the estimated results of the measured peptides OP-145 (A), P148 (B) and I12K (C) with all concentrations were presented as the percentage of PI-positive cells during time.

OP-145 show 65 % PI-positive *E. coli* K12 5K cells at a peptide concentration of 6.4 μM whereas at the killing concentrations of 1.6 – 3.2. μM only 30 – 35 % of the cell membranes were permeabilized (Figure 8A, right panel). Also in these cells P148 permeabilized the *E. coli* membranes within 5 minutes at a concentration of 0.8 μM (Figure 8B, right panel). In measurements using I12K 60 % of the cells were PI-positive at 6.4 μM peptides concentration and about 43 % at a peptide concentration of 3.2 μM (Figure 8C, right panel).

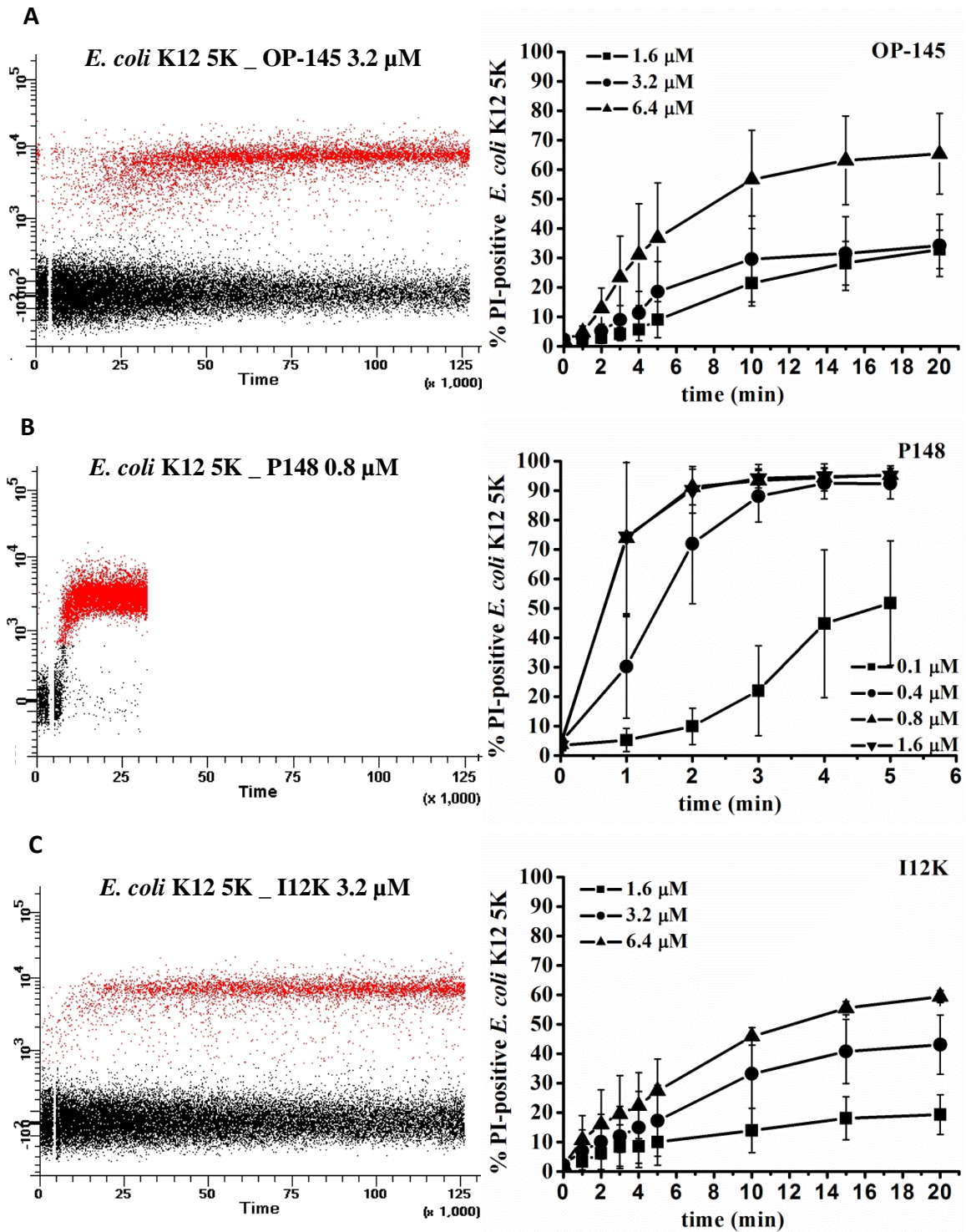


Figure 8: Membrane permeabilization in *E. coli* K12 5K by the peptides (A) OP-145, (B) P148 and (C) I12K. Propidium iodide influx (left panel) and quantification of PI-positive *E. coli* (right panel). The peptides were added after 30 seconds and PI-fluorescence was measured during 20 minutes for OP-145 and I12K, and 5 minutes for P148. The percentage of PI-positive *E. coli* was calculated at different time intervals after addition of 1.6 - 6.4 μ M OP-145 and I12K and 0.1 - 1.6 μ M P148. Results are means of three independent experiments. Time point 6 in the scale of the left panels represents one minute.

2.2 Permeabilization of model membranes mimicking bacterial membrane composition

Earlier studies showed that OP-145 (Malanovic et al., 2015) and its parent peptide, LL 37 (Sevcsik et al., 2008) preferentially interact with the anionic phospholipid phosphatidylglycerol (PG).

In this study the interaction of OP-145, P148 and I12K with model membrane systems mimicking the cytoplasmic membrane of *E. coli*, such as POPG/POPE (1:3), POPG/POPE/TMCL (20/60/10), *E. coli* polar and total lipid extract, was investigated using fluorescence based leakage experiments. The changes of the fluorescence intensity could be followed in real-time before and after the addition of incremental amounts of peptide ranging from 0.13 up to 16 μM . Physiological important concentrations of peptides are between 0.13 – 4 μM (marked with a light purple rectangle in Figure 9).

The peptides OP-145 and I12K seem not to affect the permeability of the large unilamellar vesicles because the increase of fluorescence intensity upon increasing peptide concentration was negligible (Figure 9). The only peptide which induced leakage of LUVs was P148 which differed depending on lipid composition. At the highest concentration measured (16 μM) a leakage of POPG/POPE liposomes of 65 %, 87 % for POPG/POPE/TMCL liposomes, 58 % for *E. coli* polar lipids and 79 % leakage for *E. coli* total lipids was detected. Looking at the fluorescence emission at 4 μM P148, a concentration of physiological relevance, we obtained 40 % leakage of POPG/POPE and 51 % leakage of POPG/POPE/TMCL. Membrane models composed of *E. coli* polar lipids show 21 % and *E. coli* total lipids 67 % leakage.

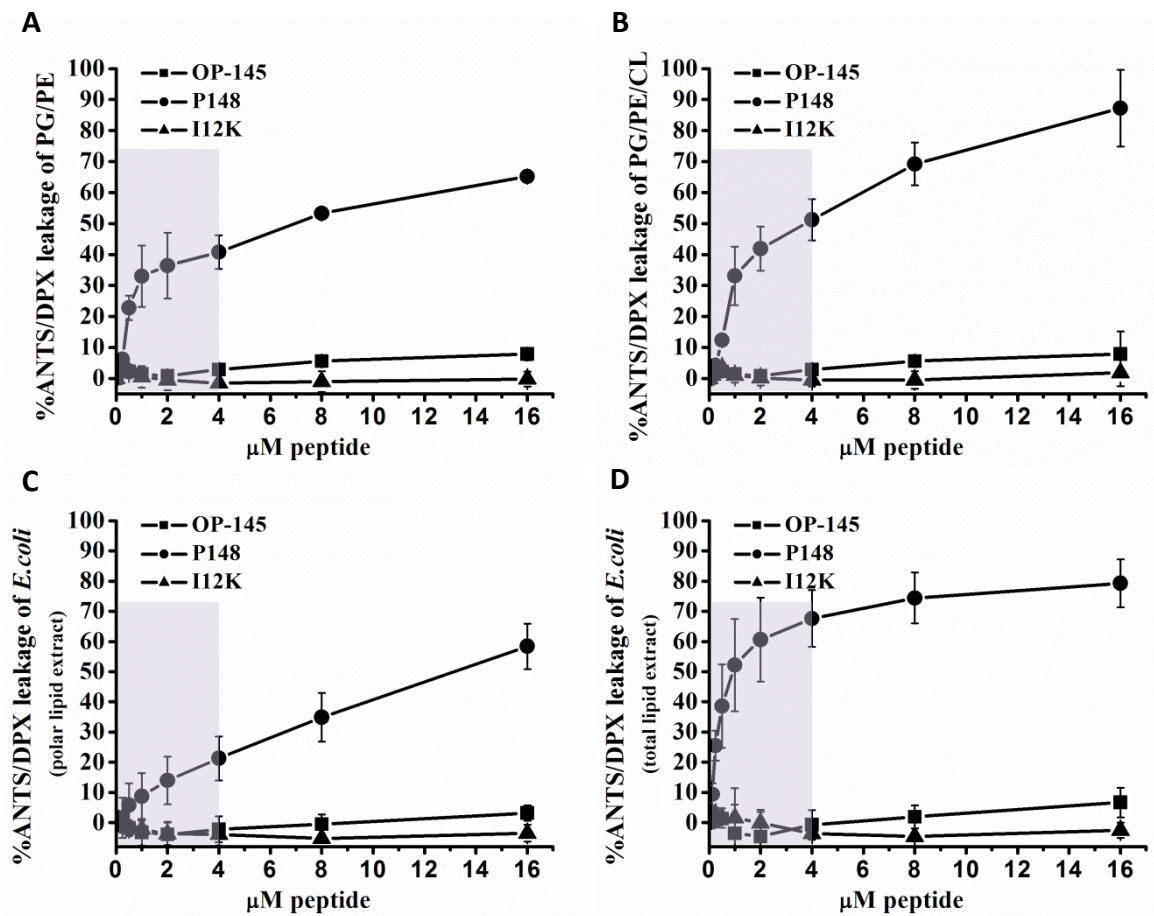


Figure 9: Effects of the peptides OP-145, P148 and I12K on bacterial model membranes measured by fluorescence leakage experiment. 50 μM liposomes were incubated with incremental amounts of peptide ranging from 0.13 up to 16 μM , corresponding to peptide-to-lipid molar ratios from 1:400 to 1:3.1. Leakage was tested with liposomes composed of (A) POPG/POPE = 1:3 (B) POPG/POPE/TMCL = 20/60/10 (C) *E. coli* polar lipid extract and (D) *E. coli* total lipid extract. Physiological important concentrations (0.13 – 4 μM peptide) are marked with a light purple rectangle.

3. Interaction with Gram-negative bacterial model membranes

Membrane permeabilization either of living *E. coli* cells or of model membranes was observed to different degrees. Therefore in order to gain further information on lipid-peptide interaction differential scanning calorimetry was performed. In order to elucidate the impact of fatty acid composition (saturated vs. unsaturated) two different model systems were used.

3.1 Thermodynamic studies with model membranes composed of phospholipids with saturated fatty acids

The interaction of the peptides OP-145, P148 and I12K with liposomes composed of DPPG/DPPE (1:3) and DPPG/DPPE/TMCL (20/60/10) was assessed by DSC at a molecular lipid to peptide ratio of 100:1 and 25:1. Figure 10 shows a comparison of scans after baseline correction and normalization. Thermodynamic parameters which were calculated by peak integration are listed in Table 4.

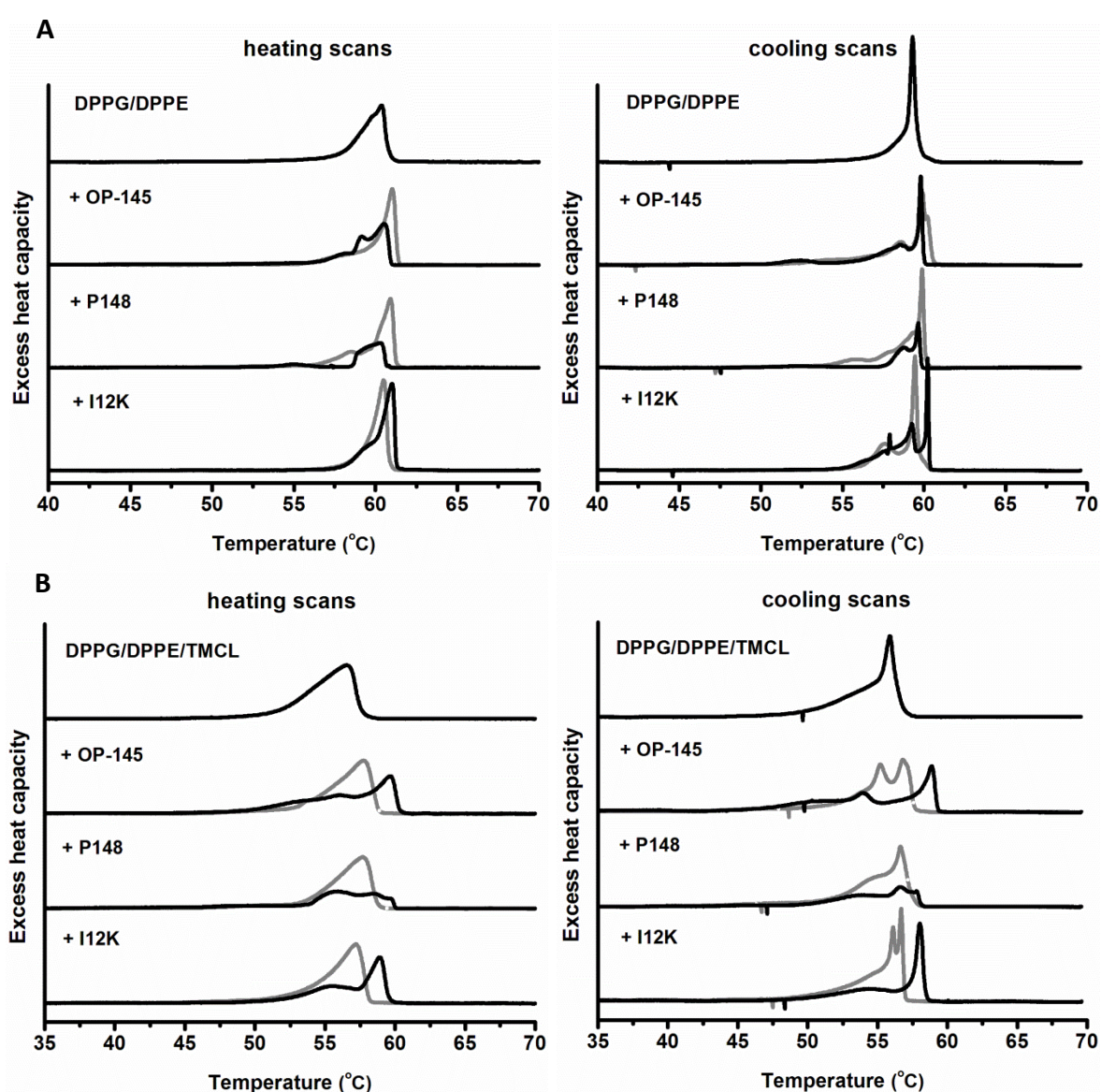


Figure 10: Interaction between the peptides OP-145, P148 and I12K with model membranes composed of (A) DPPG/DPPE and (B) DPPG/DPPE/TMCL. In the left panel the heating scans were shown and in the right panel the cooling scans. Grey lines indicate molar lipid : peptide ratio of 100:1 and the black lines lipid : peptide ratio 25:1.

Table 4: Thermodynamic parameters (phase transition temperature (T_m), half-width of transition ($\Delta T_{1/2}$) and corresponding enthalpies) of DPPG/DPPE and DPPG/DPPE/TMCL liposomes in the absence and presence of the peptides OP-145, P148 and I12K in different molecular ratios.

	Heating scans			Cooling scans		
	Enthalpy [kcal/mol]	T_m [°C]	$\Delta T_{1/2}$ [°C]	Enthalpy [kcal/mol]	T_m [°C]	$\Delta T_{1/2}$ [°C]
DPPG/DPPE	9.2	60.4	1.6	7.9	59.3	0.4
+ OP-145 (100:1)	8.4	61	0.8	8.9	59.9	0.7
+ OP-145 (25:1)	7.5	60.6	1.9	1 5.9	52.4 59.8	2.9 0.2
+ P148 (100:1)	8.9	60.9	0.9	8.6	59.9	0.3
+ P148 (25:1)	0.9 3	55.1 60.3	1.9 1.7	0.6 2.9	52.4 59.7	4.6 0.3
+ I12K (100:1)	8.3	60.5	0.8	3.7 4.6	57.6 59.5	1.6 0.3
+ I12K (25:1)	8.7	61	0.8	8.83	60.2	0.1
DPPG/DPPE/TMCL	11.1	56.5	3.4	10.5	55.9	1.1
+ OP-145 (100:1)	9.8	57.8	2.9	9.8	56.8	2.8
+ OP-145 (25:1)	9.5	59.6	2.2	0.7 8.8	39 58.9	8.5 1
+ P148 (100:1)	9.3	57.7	2.8	9.9	56.6	2.1
+ P148 (25:1)	1.2 4.6	49.5 55.9	6.1 5.5	5	56.7	5
+ I12K (100:1)	0.2 10.2	39.7 57.2	3.6 2.5	0.6 9.9	38.8 56.7	9.2 1
+ I12K (25:1)	0.1 7.5	39.9 58.9	6.1 1.3	0.5 6.8	38.1 58.2	7.6 0.5

The thermotropic phase behavior of both model systems was characterized by a phase transition from the gel to the fluid phase at 60.4 °C for DPPG/DPPE and for DPPG/DPPE/TMCL at 56.5 °C. Upon cooling from the fluid to the gel phase a shift of the main transition to 59.3 °C for DPPG/DPPE and 55.9 °C for DPPG/DPPE/TMCL was observed (Figure 10, Table 4).

Pure DPPG has a main transition temperature at 41.5 °C, DPPE at 63.4 °C (Sevesik et al., 2008; Karl Lohner, 2016) and pure TMCL around 41 °C (Prossnigg et al., 2010). All antimicrobial peptides induce a shift of the main transition temperature (T_m). Analysis of both model membranes (Figure 10, Table 4) showed that most of the peptides induce an

increase of the main transition temperature at the molar lipid to peptide ratio of 100:1 with a decrease of the half-width of transition. An increasing T_m means a stabilization of the gel phase due to a tighter lipid packing. With increasing peptide concentration (molar ratio of 25:1) domain formation melting at different temperatures were observed. Depending on the peptide and its concentration the phases are separated totally from each other or overlapped (Figure 10). The thermodynamic parameters of former are listed as distinct data. Overlapping domains did not allow calculating accurately their respective enthalpies and therefore the total enthalpy of the system is given.

OP-145 shows a slight decrease of the total enthalpy and the formation of new domains which were not fully separated from each other. The effect is more pronounced with P148 as deduced from the clearly separated domains and the decrease of the enthalpy by 50 %. I12K is the peptide which shows the least effect in the heating scans. In the DPPG/DPPE system only the appearance of a shoulder at the low temperature side is observed, which is more obvious in the model membranes including TMCL.

Domain formation is detected more clearly in the cooling scans of the DPPG/DPPE (1:3) and DPPG/DPPE/TMCL (20/60/10) mixtures characterized by a smaller transition half-width indicating a higher cooperativity.

It can be expected that domains which contain more DPPE are shifted to higher and domains with an increasing DPPG content to lower phase transition temperatures. AMPs because of their positive charge will more likely interact with the negatively charged DPPG and hence will be enriched in these domains (Malanovic et al., 2015; Karl Lohner, 2016).

3.2 Thermodynamic studies with model membranes composed of phospholipids with (un)saturated fatty acids

The interaction of the peptides OP-145, P148 and I12K with liposomes composed of POPG/POPE (1:3) and POPG/POPE/TMCL (20/60/10) was assessed by DSC at a molecular lipid to peptide ratio of 25:1 (Figure 11). In contrast to DPPG and DPPE these lipids have unsaturated fatty acids in position 2 which results in a lower phase transition temperature (T_m) and a lower enthalpy, the half-width of transition ($\Delta T_{1/2}$) however increases due to lower cooperativity (Table 5). Both model systems are characterized by a phase transition from the gel phase to the fluid phase at 21.1 °C for POPG/POPE and at 26 °C for POPG/POPE/TMCL. Pure POPG has a main transition temperature around -5 °C (Pozo Navas et al., 2005) and pure POPE at about 24 °C (Koynova and Caffrey, 1994; Rappolt et al., 2003).

Antimicrobial peptides have a disordering effect on POPG/POPE model membranes which is clearly visible by the domain formation observed for all peptides used (Figure 11A). This separation is again more clearly detected in the cooling scans (listed separately in Table 5).

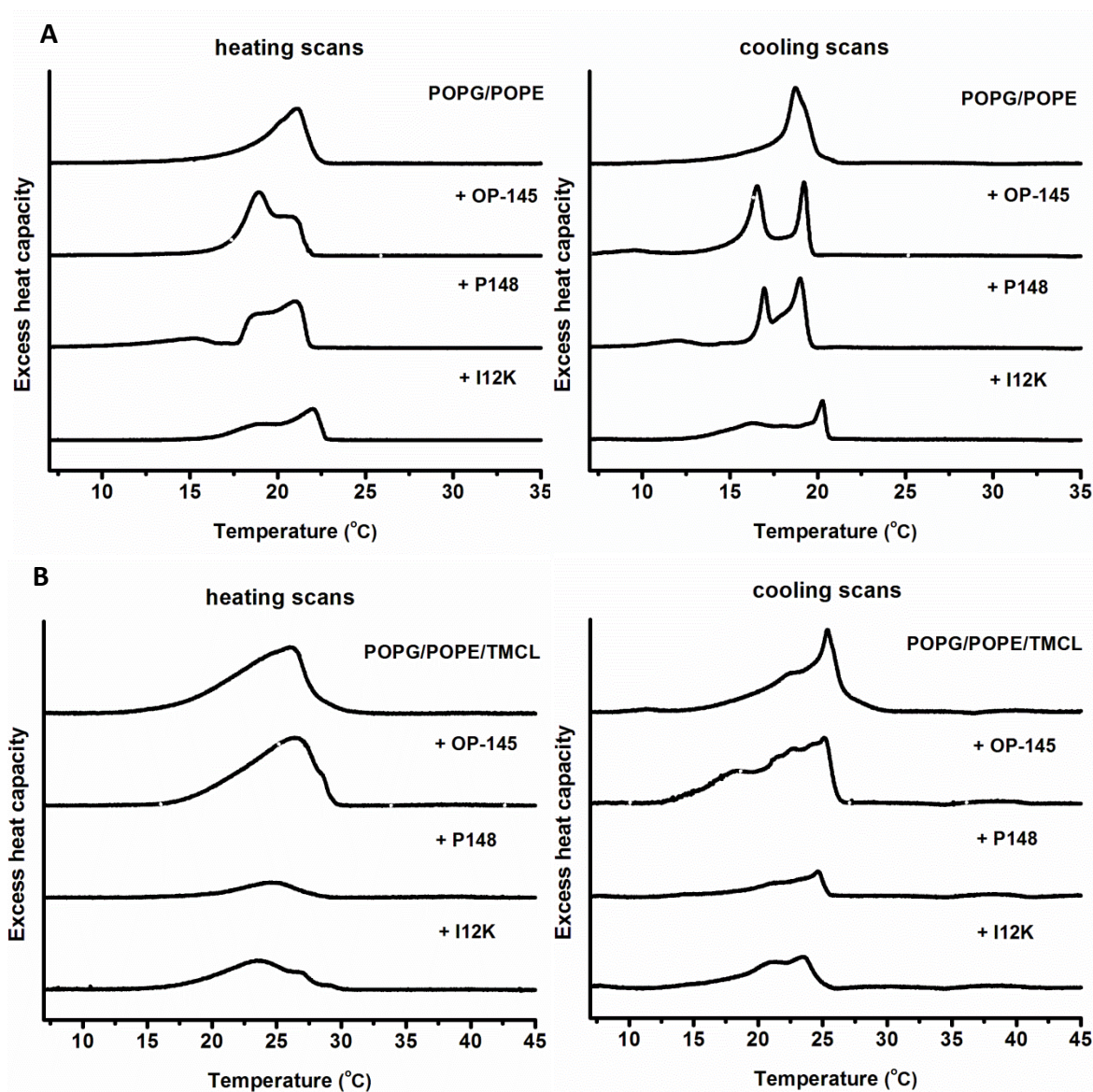


Figure 11: Interaction between the peptides OP-145, P148 and I12K with model membranes composed of (A) POPG/POPE and (B) POPG/POPE/TMCL. In the left panel the heating scans are shown and in the right panel the cooling scans. Measurements were done with a lipid : peptide ratio of 25:1.

OP-145 leads to an increase of the total enthalpy but does not induce full separation of the domains. P148 also increases the total enthalpy but induces formation of three domains, where the low melting one (15.1 °C) is enriched in POPG. I12K also induces domain formation however with a decreased total enthalpy of 3.4 from 5.8 kcal/mol. OP-145 and P148 decrease the main transition temperature, whereas I12K increases the main transition temperature in the heating and in the cooling scan (Table 5).

Table 5: Thermodynamic parameters (phase transition temperature (T_m), half-width of transition ($\Delta T_{1/2}$) and corresponding enthalpies) of POPG/POPE and POPG/POPE/TMCL liposomes in the absence and presence of the peptides OP-145, P148 and I12K, lipid : peptide molar ratio of 25:1.

	Heating scans			Cooling scans		
	Enthalpy [kcal/mol]	T_m [°C]	$\Delta T_{1/2}$ [°C]	Enthalpy [kcal/mol]	T_m [°C]	$\Delta T_{1/2}$ [°C]
POPG/POPE	5.8	21.1	2.4	5.3	18.7	1.4
+ OP-145 (25:1)	6.4	18.9	3.3	0.6	9.5	3.9
				3.5	16.5	0.9
+ P148 (25:1)	1.5	15.1	4	2	19.2	0.6
				0.9	12	3.1
				1.8	17	0.6
+ I12K (25:1)	4.5	20.9	3.4	2.9	19	1.2
				3.4	22	3.7
POPG/POPE/TMCL	7.6	26	6.2	5.7	25.4	2.6
+ OP-145 (25:1)	7.2	26.4	6.2	7.3	25.1	5.6
+ P148 (25:1)	1.4	24.4	5	1.6	24.6	4.1
+ I12K (25:1)	3.4	23.5	7	2.8	23.4	4.9

The effect of the AMPs is different for the POPG/POPG/TMCL model membranes. Here we can see a disordering effect lowering the cooperativity for all peptides OP-145, P148 and I12K as deduced from the broad phase transition in both heating and cooling scans. P148 shows a dramatic decrease of the enthalpy of about 80 % and I12K a decrease of about 50 %. Both peptides also induce a decrease of the phase transition temperature. OP-145 had less effect on the thermodynamic parameters in the heating scan, whereas in the cooling scan it leads to an increase of the enthalpy and the half-width of transition.

4. Lipid domain formation *in vivo* induced by AMPs

To see effects on the membrane of *E. coli*, which were incubated with antimicrobial peptides, the cells were examined under a fluorescence microscope after a lipophilic Nile red stain. For these experiments peptide concentrations 2-3 x lower than their lethal concentration for 5×10^7 cells were chosen. Untreated and 20 minutes with peptide incubated *E. coli* ATCC 25922 cells are shown in Figure 12 and *E. coli* K12 5K cells in Figure 13. The intensities of the microscopy pictures are dependent on the adjusted intensity during the recordings, which changed depending on the sample and intensity of the stain.

The untreated cells had a homogenous distribution of the stain through the whole cell membrane (Figure 12 and 13). After incubation with peptide first larger lipid domains were formed at both poles of the cells which is shown in the first panel of the Figures 12 and 13. *E. coli* ATCC 25922 was incubated with 12.8 – 25.6 μM OP-145, 3.2 – 6.4 μM P148 and 25.6 – 102.4 μM I12K whereas *E. coli* K12 5K was incubated with 6.4 – 12.8 μM OP-145, 3.2 – 12.8 μM P148 and 12.8 – 51.2 μM I12K. At a higher peptide concentration the formation of smaller lipid domains was detected also in other parts of the cell. Such formation of lipid domains in *E. coli* ATCC 25922 was best observed in the case of I12K at the peptide concentrations between 25.6 and 51.2 μM (Figure 12 lowest panel), which resulted in death at 102.4 μM .

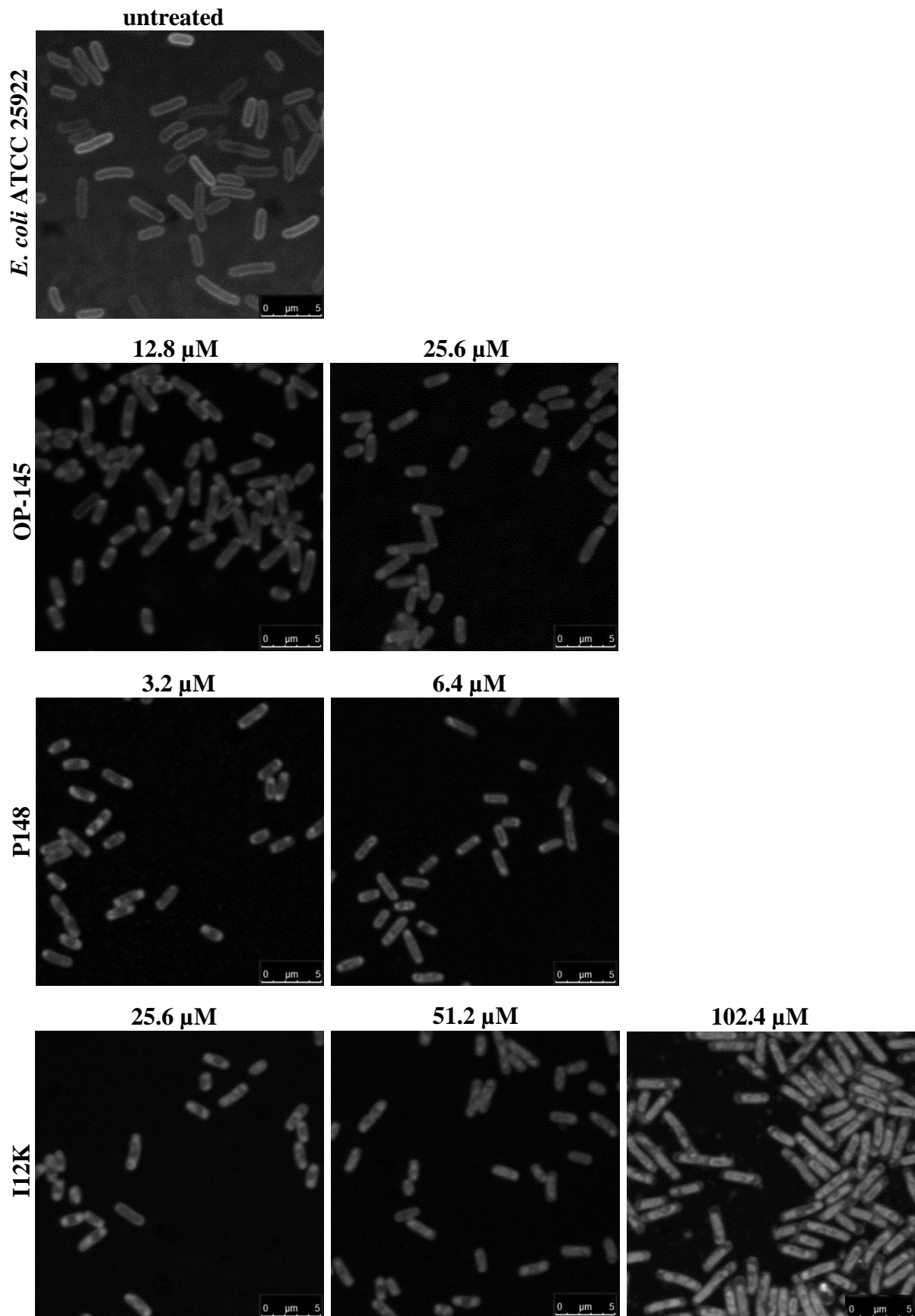


Figure 12: Antimicrobial peptides trigger lipid domain formation *in vivo*. Fluorescence images of *E. coli* ATCC 25922 cells stained with Nile red untreated and after incubation with 12.8 – 25.6 μM OP-145, 3.2 – 6.4 μM P148 and 25.6 – 102.4 μM I12K for 20 minutes at 37 °C. Typical figures are shown.

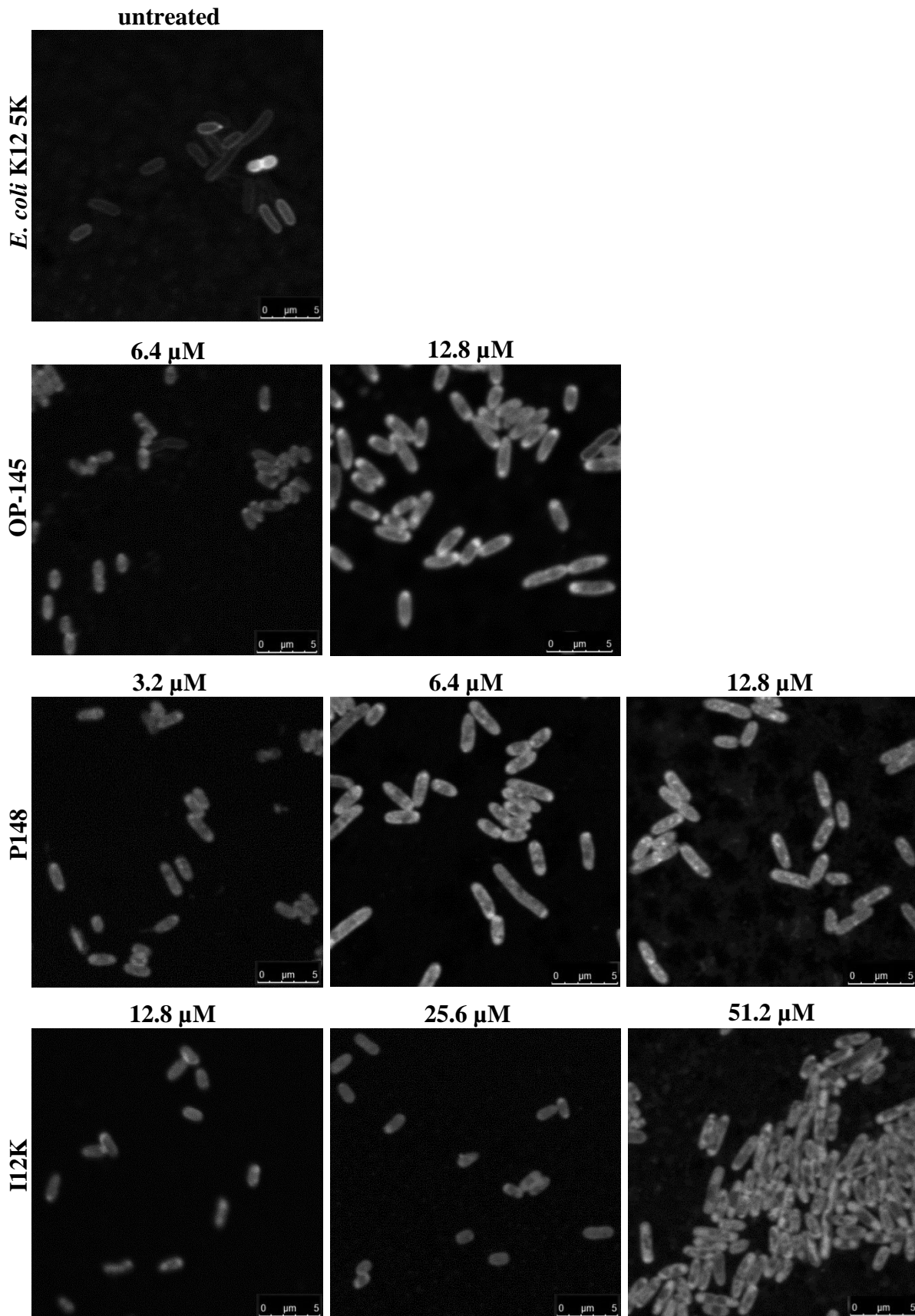


Figure 13: Antimicrobial peptides trigger lipid domain formation *in vivo*. Fluorescence images of *E. coli* K12 5K cells stained with Nile red untreated and after incubation with 6.4 – 12.8 μM OP-145, 3.2 – 12.8 μM P148 and 12.8 – 51.2 μM I12K for 20 minutes at 37 °C. Typical figures are shown.

IV. DISCUSSION

A general mechanism of bacterial killing by cationic antimicrobial peptides is thought to be targeting the anionic phospholipids on the membrane surface, which leads to membrane disruption or damage and in turn to cell death (Lohner, 2009). Besides the zwitterionic PE which is the main component of Gram-negative bacteria the plasma membrane also contains the negatively charged PG, while zwitterionic PC is the major component of mammalian outer membrane. There are several studies concerning the interaction of antimicrobial peptides like OP-145 with model membranes mimicking bacterial and mammalian cell membranes (Malanovic et al., 2015).

The main aim of this thesis was to determine the membrane permeabilization activity of the peptides OP-145, P148 and I12K towards living and model Gram-negative bacterial membranes using several methods. As representatives of the Gram-negative bacteria two different aerobic *Escherichia coli* strains with the biosafety level 1 were used. *E. coli* ATCC 25922 (also *E. coli* (Migula) Castellani and Chalmers) is a strain approved by the Food and Drug Administration (FDA) for antibiotic and antimicrobial susceptibility testing which does not produce verotoxin. *E. coli* K12 5K is a wild-type laboratory strain derived from the *E. coli* K-12 family which represents the genetically best understood living organism. The K-12 strains are devoid of all known *E. coli* virulence genes and are therefore considered to be a prototype of safe and nonpathogenic bacterial strains. The most important difference of the *E. coli* K-12 strain from other *E. coli* strains is the lack of the O antigen, which is part of the lipopolysaccharide, due to a mutation of a gene which leads to the inactivation of a key enzyme in the O antigen biosynthesis (Kuhnert et al., 1995).

The first task of this work was to identify the lethal concentration ($LC_{99.9}$ = lowest peptide concentration that results in > 99.9 % killing of *E. coli*) of the used peptides against these two

strains by a standard killing assay. For this approximately 1×10^6 CFU/ml of NaPi (20 mM NAPI, 130 mM NaCl, pH 7.4) were used as a standard cell concentration.

The originally LL-37 derived peptide OP-145 shows similar activities against both *E. coli* strains which were killed at $3.2 \mu\text{M}$ within 20 minutes. However, real-time experiments based on propidium iodide (PI), a non-permeable fluorescent dye, which is indicative for permeabilization of *E. coli* membranes after incubation with peptides, showed marked difference to the killing assay on agar plates. Cells only get PI-positive, when the membrane gets damaged by the peptides enabling translocation of propidium iodide through the membrane and binding to the DNA of the bacteria resulting in fluorescence. At a concentration of $3.2 \mu\text{M}$ OP-145 only 26 % of the *E. coli* ATCC 25922 cells (Figure 7) and 35 % of the *E. coli* K12 5K cells (Figure 8) were PI-positive after 20 minutes peptide incubation. This means that at the time point of the cell death determined by the killing assay on agar plates the membrane of the bacteria is not totally permeabilized. Seemingly OP-145 perturbs the membrane in a way that the bacterial strains are not able to grow. Most of the cells are not dead due to membrane lysis, but they cannot grow and form colonies as shown by the killing assay on the plates (Figure 5).

The highest activity was shown by the peptide P148, developed from OP-145, which has a net charge of +11 at physiological pH compared to OP-145 which has a net charge of +6. P148 was designed in a way to have improved amphipathic character which results in a killing of *E. coli* cells within 5 minutes at a concentration of $0.8 \mu\text{M}$. In comparison to OP-145 this killing was also observed with the fluorescence based PI-experiment which also showed permeabilization of the *E. coli* membrane within five minutes at the same peptide concentration. The peptide was also very effective against living cells at a concentration of $0.4 \mu\text{M}$ (Figure 5, 7 and 8). Killing of the cells is induced by the instant permeabilization of the *E. coli* plasma membrane. Thus the high activity of P148 is most likely due to the higher

positive charge of the small helical peptide which can stronger interact with the negatively charged bacterial plasma membrane.

If we look at the killing which was induced by I12K, also developed from OP-145, we observed marked differences between the two *E. coli* strains compared to the other two peptides. While the *E. coli* K12 5K cells were killed in 20-30 minutes at the concentration of 3.2 μM I12K for the ATCC 25922 strain a higher peptide concentration was needed. With 25.6 μM I12K it takes about 5 minutes to kill all bacteria and at 12.8 μM 99 % death was reached after 5 minutes, but it took up to 2 hours to reach the $\text{LC}_{99.9}$. Like OP-145 also this peptide did not show full membrane permeabilization at the real-time experiment with *E. coli* cells. *E. coli* ATCC 25922 reaches a permeabilization rate of 90 % after 20 minutes incubation with I12K which increases insignificantly after the tenth minute. Considering *E. coli* K12 5K at the lethal concentration of 3.2 μM only 43 % of the cells were dead after 20 minutes due to membrane permeabilization. This means that not even half of the bacteria which did not show growth on agar plates after 20 minutes were dead at the same time point. These results are similar to the measurements with OP-145. Also this peptide damages the cell membrane in a way that the bacteria cannot survive and form colonies on agar plates. Therefore, we suggest that killing took not instantly place which leads to a much lower percentage of PI-positive cells than expected from the killing concentration of the peptide determined on the agar plates.

The variable activity of I12K between the two strains could have several reasons. It is important to mention that before the peptides can bind to the plasma membrane they have to cross the outer membrane which is a lipid bilayer, where the inner leaflet is composed of phospholipids and the outer leaflet of lipopolysaccharides (LPS) in Gram-negative bacteria (Figure 1). LPS in Gram-negative strains may have the similar function as its counterpart lipoteichoic acid (LTA) in Gram-positive bacteria (Malanovic and Lohner, 2016). The *E. coli* K12 5K strain in comparison to *E. coli* ATCC 25922 lacks the O-antigen which is a part of

the LPS structure. This could lead to a less densely packed outer layer which then facilitates crossing of the peptides as compared to the outer membrane of *E. coli* ATCC 25922 cells resulting in higher activity of I12K against the K12 5K strain. Furthermore, this peptide has in comparison to OP-145 and P148 a kink in the α -helix which is caused by a basic polar amino acid between the hydrophobic ones (Figure 4). Because of this structural difference I12K may have different binding capacity to the two LPS reducing the effective concentration at the plasma membrane to various extents. This in turn may lead to a reduced activity against the *E. coli* ATCC 25922 cells.

To sum up the observations in Figures 7 and 8 we can say that there is an increase of PI-positive cells with increasing peptide concentration, but the percentage of the measured dead cells is not as high as expected due to the killing concentration of the peptides OP-145 and I12K determined by the killing assay on agar plates. The only exception is P148 which shows full permeabilization of the *E. coli* cell membranes in agreement with killing time.

Besides the membrane permeabilization activity of the peptides on *E. coli* cells the permeabilization was also measured with liposomes consisting of the major phospholipids of Gram-negative bacterial strains like PG, PE and CL and membrane extracts of *E. coli* (results shown in Figure 9). Focusing on the physiological important peptide concentrations (peptide-to-lipid molar ratio up to 1:12.5, marked with a light purple rectangle in Figure 9) OP-145 and I12K induce negligible membrane permeabilization of all four tested membrane models. The highest activity however was shown by P148 with about 67 % leakage for model membranes prepared with the *E. coli* total lipid extract that contains besides the three major phospholipid components also an unknown part of 17.6 % which is most likely LPS. This may point to stronger interaction of P148 with LPS facilitating membrane permeabilization. Also, an increase of leakage by 10 % at CL containing liposomes as compared to liposomes containing only PE and PG, which is also higher than in liposomes composed of *E. coli* polar lipid

extract that also contain PE, PG and CL, was observed. However, 100 % leakage was not reached in any of the tested liposomes even at the highest measured peptide concentration.

As previously reported, OP-145 is able to permeabilize fully large unilamellar vesicles composed of POPG at a peptide concentration of 4 μM . Whereas 50 % membrane leakage was already obtained at a total concentration of 1 μM OP-145 for POPG vesicles, this value was not reached for non-charged POPC vesicles even at the highest tested OP-145 concentration (Malanovic et al., 2015). Gram-negative bacteria, such as *E. coli*, have a 3 times higher PE amount than PG in their plasma membranes which leads to a lower negative net charge than in Gram-positive bacteria, where the negatively charged PG is the major component of the cytoplasmic membrane (Malanovic and Lohner, 2016). This could be also a reason for the reduced activity of the peptides OP-145 and I12K as well as of P148 observed for model membranes mimicking Gram-negative bacterial plasma membranes. An important difference between P148 and the other two peptides is that the total positive net charge of P148 is higher than in OP-145 and I12K which leads to a stronger interaction with negatively charged membrane components like PG and CL. Regarding the low leakage values as compared to membrane permeabilization of living cells suggests that other structures in bacterial membranes help the antimicrobial peptides to bind and perturb the cell membrane leading to cell death. The problematic of correlation between antimicrobial activity and vesicle permeabilization has been already discussed in detail (Wimley, 2010).

Differential scanning calorimetry (DSC) measurements of model membranes showed that all three peptides interact with PG/PE (25:75) and PG/PE/CL (20/60/10) liposomes (Figure 10 and 11). DSC measurements using a molar lipid to peptide ratio of 25:1 can be compared with the leakage measurements using 2 μM peptides. At this peptide concentration domain formation was observed by DSC for all peptides. However, only P148 markedly reduced the transition enthalpy indicating a strong destabilization of the membrane. This correlates well

with the fact that significant leakage of entrapped fluorescence marker molecules was only observed for this peptide.

DSC is a method which is widely used for phase transition studies and conformational changes in biological systems, including nucleic acids, proteins and lipid assemblies. From a single calorimetric scan it is possible to determine thermodynamic information like transition temperature (T_m), transition enthalpy and cooperativity. The transition half-width ($\Delta T_{1/2}$) is often used as a qualitative measure of cooperativity (Karl Lohner, 2016). Here, the DSC measurements were performed using lipids composed of saturated fatty acids (Figure 10) and unsaturated fatty acids (Figure 11). The figures show that the peaks in the cooling scans are sharper in comparison to the heating scans relating to higher cooperativity of the transition upon cooling. In order to gain information on the effect of different peptide concentrations dipalmitoyl-PG and -PE vesicles were prepared with a molar lipid to peptide ratio of 100:1 and 25:1. The presence of lower peptide amounts (100:1) stabilized the gel phase as deduced from an increase of the main transition temperature. With increasing peptide concentration (molar ratio of 25:1) we observed domain formation with different phase transition temperatures (Table 4 and 5). TMCL containing DPPG/DPPE vesicles gave similar results but with a stronger separation of the formed lipid domains (Figure 10B). The domain separation is more clearly detected in the cooling scans than in the heating scans. Considering the effects of the peptides on POPG/POPE liposomes it has been shown that they interact in a quite similar way, i.e. formation of new lipid domains. An important point to consider is however that vesicles composed of POPG/POPE/TMCL (Figure 11B) did not show a clear separation of the lipid domains induced by the peptides in contrast to DPPG/DPPE/TMCL. It is known that the positively charged peptides preferentially bind to negatively charged lipids. Therefore, we can assume that lipid domain with the lowest phase transition temperature (domains containing higher PG because of its lower T_m) have most of the peptides bound, whereas domains with higher T_m will be enriched in PE and depleted in antimicrobial peptides.

Domain formation detected in the DSC experiments was also visible in both *E. coli* strains under the fluorescence microscope after staining with the lipophilic dye Nile Red (Figure 12 and 13). Untreated *E. coli* have a homogeneous distribution of the lipids within the membrane around the cells. After incubation of the cells with antimicrobial peptides lower than their lethal concentration, large lipid domains are formed at the poles of the *E. coli* cells. When the concentration of the peptides is increased smaller lipid domains are visible over the whole bacteria. It is important to note, that amount of the used bacterial cells vary in different experiments. Therefore, as the antimicrobial activity does not increase in a linear way with increasing amount of bacteria (Roversi et al., 2014), the killing concentration was adjusted accordingly. Despite of the strong variation of the effects of the peptides in different *E.coli* strains and performed experiments, domain formation at the poles of the cells is observed with all peptides. Scheinpflug et al. observed similar domain formation in *Bacillus subtilis* upon incubation with *cWFW* peptide which is accompanied with defects in membrane protein deorganization triggering autolysis (Scheinpflug et al., 2017). However, *cWFW* peptide did not induce membrane permeabilization neither in living bacteria nor in model membranes like peptides in this study.

To conclude, all peptides used had a similar mode of action to Gram-negative bacterial strains and also in calorimetric measurements with model membranes; only the concentration of the peptide to achieve a certain effect is different. Whereas P148 kills bacteria very fast inducing instant membrane permeabilization, OP-145 and I12K are inducing killing in a slower way and at a higher peptide concentration. These peptides also did not permeabilize instantly the cytoplasmic membrane. Whatever the exact mechanism is, interaction with phospholipids and formation of lipid domains initiate the process of killing. Although there are several clinical studies for OP-145, based on this study P148 seems to be an improved candidate for further bacterial and mammalian studies for the development of a new antimicrobial agent.

ABBREVIATIONS

AMP	antimicrobial peptide
ANTS	8-aminonaphthalene-1.3.6-trisulfonic acid
ATCC	American Type Culture Collection
BAI	biomaterial-associated infections
CFU	colony forming units
CL	cardiolipin
DPPE	1,2-dipalmitoyl- <i>sn</i> -glycero-3-phosphoethanolamine
DPPG	1,2-dipalmitoyl- <i>sn</i> -glycero-3-phospho- <i>rac</i> -glycerol
DPX	p-xylene-bis-pyridinium bromide
DSC	differential scanning calorimetry
<i>E. coli</i>	<i>Escherichia coli</i>
FDA	Food and Drug Administration
I12K	antimicrobial peptide developed from OP-145
LC	lethal concentration (99.9 % cell death)
LL-37	AMP from the human cathelicidin family, released from the precursor hCAP18
LPS	lipopolysaccharide
LTA	lipoteichoic acid
LUV	large unilamellar vesicle
MHB	Mueller Hinton Broth
MRSA	methicillin-resistant <i>S. aureus</i>
NaPi	sodium phosphate buffer
OD	optical density
OP-145	antimicrobial peptide derived from LL-37
P148	antimicrobial peptide developed from OP-145

PC	phosphatidylcholine
PE	phosphatidylethanolamine
PG	phosphatidylglycerol
PI	propidium iodide
POPE	1-palmitoyl-2-oleoyl- <i>sn</i> -glycero-3-phosphoethanolamine
POPG	1-palmitoyl-2-oleoyl- <i>sn</i> -glycero-3-phospho- <i>rac</i> -glycerol
PS	phosphatidylserine
RT	room temperature
<i>S. aureus</i>	<i>Staphylococcus aureus</i>
SM	sphingomyelin
$\Delta T_{1/2}$	half-width of transition
T_m	phase transition temperature
TMCL	1,1',2,2'-tetramyristoyl cardiolipin

REFERENCES

- Andrès, E. (2012). Cationic antimicrobial peptides in clinical development, with special focus on thanatin and heliomicin. In: *European Journal of Clinical Microbiology & Infectious Diseases* 31 (6), S. 881–888. DOI: 10.1007/s10096-011-1430-8.
- Bechinger, Burkhard; Lohner, Karl (2006). Detergent-like actions of linear amphipathic cationic antimicrobial peptides. In: *Biochim. Biophys Acta* 1758 (9), S. 1529–1539. DOI: 10.1016/j.bbamem.2006.07.001.
- Boman, H. G. (2003). Antibacterial peptides. Basic facts and emerging concepts. In: *Journal of internal medicine* 254 (3), S. 197–215.
- Breij, A. de; Riool, M.; Kwakman, P.H.S.; Boer, L. de; Cordfunke, R. A.; Drijfhout, J. W. et al. (2016). Prevention of Staphylococcus aureus biomaterial-associated infections using a polymer-lipid coating containing the antimicrobial peptide OP-145. In: *Journal of Controlled Release* 222 (Supplement C), S. 1–8. DOI: 10.1016/j.jconrel.2015.12.003.
- Broekhuysse, R. M. (1968). Phospholipids in tissues of the eye I. Isolation, characterization and quantitative analysis by two-dimensional thin-layer chromatography of diacyl and vinyl-ether phospholipids. In: *Biochimica et Biophysica Acta (BBA) - Lipids and Lipid Metabolism* 152 (2), S. 307–315. DOI: 10.1016/0005-2760(68)90038-6.
- Burton, Matthew F.; Steel, Patrick G. (2009). The chemistry and biology of LL-37. In: *Natural Product Reports* 26 (12), S. 1572–1584. DOI: 10.1039/B912533G.
- Chen, Fang-Yu; Lee, Ming-Tao; Huang, Huey W. (2003). Evidence for membrane thinning effect as the mechanism for peptide-induced pore formation. In: *Biophysical journal* 84 (6), S. 3751–3758. DOI: 10.1016/S0006-3495(03)75103-0.
- Durr, Ulrich H. N.; Sudheendra, U. S.; Ramamoorthy, Ayyalusamy (2006). LL-37, the only human member of the cathelicidin family of antimicrobial peptides. In: *Biochim. Biophys Acta* 1758 (9), S. 1408–1425. DOI: 10.1016/j.bbamem.2006.03.030.
- Fjell, Christopher D.; Hiss, Jan A.; Hancock, Robert E. W.; Schneider, Gisbert (2011). Designing antimicrobial peptides. Form follows function. In: *Nature reviews. Drug discovery* 11 (1), S. 37–51. DOI: 10.1038/nrd3591.
- Haisma, Elisabeth M.; Breij, Anna de; Chan, Heelam; van Dissel, Jaap T.; Drijfhout, Jan W.; Hiemstra, Pieter S. et al. (2014). LL-37-derived peptides eradicate multidrug-resistant Staphylococcus aureus from thermally wounded human skin equivalents. In: *Antimicrobial agents and chemotherapy* 58 (8), S. 4411–4419. DOI: 10.1128/AAC.02554-14.
- Hancock, Robert E. W. (2001). Cationic peptides. Effectors in innate immunity and novel antimicrobials. In: *The Lancet Infectious Diseases* 1 (3), S. 156–164. DOI: 10.1016/S1473-3099(01)00092-5.
- Hancock, Robert E. W.; Sahl, Hans-Georg (2006). Antimicrobial and host-defense peptides as new anti-infective therapeutic strategies. In: *Nature biotechnology* 24 (12), S. 1551–1557. DOI: 10.1038/nbt1267.

- Kahlenberg, J. Michelle; Kaplan, Mariana J. (2013). Little Peptide, Big Effects. The Role of LL-37 in Inflammation and Autoimmune Disease. In: *The Journal of Immunology* 191 (10), S. 4895. DOI: 10.4049/jimmunol.1302005.
- Karl Lohner (2016). DSC Studies on the Modulation of Membrane Lipid Polymorphism and Domain Organization by Antimicrobial Peptides. In: Margarida Bastos (Hg.): *Biocalorimetry*: CRC Press, S. 169–190.
- Koraimann, G.; Högenauer, G. (1989). A stable core region of the tra operon mRNA of plasmid R1-19. In: *Nucleic Acids Research* 17 (4), S. 1283–1298.
- Koynova, Rumiana; Caffrey, Martin (1994). Phases and phase transitions of the hydrated phosphatidylethanolamines. In: *Chemistry and Physics of Lipids* 69 (1), S. 1–34. DOI: 10.1016/0009-3084(94)90024-8.
- Kuhnert, P.; Nicolet, J.; Frey, J. (1995). Rapid and accurate identification of Escherichia coli K-12 strains. In: *Applied and Environmental Microbiology* 61 (11), S. 4135–4139.
- Latal, A.; Degovics, G.; Epanand, R. F.; Epanand, R. M.; Lohner, K. (1997). Structural aspects of the interaction of peptidyl-glycylleucine-carboxamide, a highly potent antimicrobial peptide from frog skin, with lipids. In: *European journal of biochemistry* 248 (3), S. 938–946.
- Lohner, K.; Blondelle, S. E. (2005). Molecular mechanisms of membrane perturbation by antimicrobial peptides and the use of biophysical studies in the design of novel peptide antibiotics. In: *Combinatorial chemistry & high throughput screening* 8 (3), S. 241–256.
- Lohner, K.; Latal, A.; Lehrer, R. I.; Ganz, T. (1997). Differential scanning microcalorimetry indicates that human defensin, HNP-2, interacts specifically with biomembrane mimetic systems. In: *Biochemistry* 36 (6), S. 1525–1531. DOI: 10.1021/bi961300p.
- Lohner, K., editor. (2001). *Development of Novel Antimicrobial Agents: Emerging Strategies*. Horizon Scientific Press, Wymondham, United Kingdom.
- Lohner, Karl (2009). New strategies for novel antibiotics. Peptides targeting bacterial cell membranes. In: *General physiology and biophysics* 28 (2), S. 105–116.
- Lohner, Karl (2017). Membrane-active Antimicrobial Peptides as Template Structures for Novel Antibiotic Agents. In: *Current topics in medicinal chemistry* 17 (5), S. 508–519.
- Ludtke, S. J.; He, K.; Heller, W. T.; Harroun, T. A.; Yang, L.; Huang, H. W. (1996). Membrane pores induced by magainin. In: *Biochemistry* 35 (43), S. 13723–13728. DOI: 10.1021/bi9620621.
- Malanovic, N.; Leber, R.; Schmuck, M.; Kriechbaum, M.; Cordfunke, R. A.; Drijfhout, J. W. et al. (2015). Phospholipid-driven differences determine the action of the synthetic antimicrobial peptide OP-145 on Gram-positive bacterial and mammalian membrane model systems. In: *Biochim. Biophys Acta* 1848 (10 Pt A), S. 2437–2447.
- Malanovic, Nermina; Lohner, Karl (2016). Gram-positive bacterial cell envelopes. The impact on the activity of antimicrobial peptides. In: *Biochim. Biophys Acta* 1858 (5), S. 936–946. DOI: 10.1016/j.bbamem.2015.11.004.

- Matsuzaki, K.; Murase, O.; Fujii, N.; Miyajima, K. (1996). An antimicrobial peptide, magainin 2, induced rapid flip-flop of phospholipids coupled with pore formation and peptide translocation. In: *Biochemistry* 35 (35), S. 11361–11368. DOI: 10.1021/bi960016v.
- Nell, Marja J.; Tjabringa, G. Sandra; Wafelman, Amon R.; Verrijck, Ruud; Hiemstra, Pieter S.; Drijfhout, Jan W.; Grote, Jan J. (2006). Development of novel LL-37 derived antimicrobial peptides with LPS and LTA neutralizing and antimicrobial activities for therapeutic application. In: *Peptides* 27 (4), S. 649–660. DOI: 10.1016/j.peptides.2005.09.016.
- Nguyen, Leonard T.; Haney, Evan F.; Vogel, Hans J. (2011). The expanding scope of antimicrobial peptide structures and their modes of action. In: *Trends in biotechnology* 29 (9), S. 464–472. DOI: 10.1016/j.tibtech.2011.05.001.
- Oren, Ziv; LERMAN, Jeffrey C.; GUDMUNDSSON, Gudmundur H.; AGERBERTH, Birgitta; Shai, Yechiel (1999). Structure and organization of the human antimicrobial peptide LL-37 in phospholipid membranes. Relevance to the molecular basis for its non-cell-selective activity. In: *Biochemical Journal* 341 (3), S. 501. DOI: 10.1042/bj3410501.
- Porcelli, Fernando; Verardi, Raffaello; Shi, Lei; Henzler-Wildman, Katherine A.; Ramamoorthy, Ayyalusamy; Veglia, Gianluigi (2008). NMR structure of the cathelicidin-derived human antimicrobial peptide LL-37 in dodecylphosphocholine micelles. In: *Biochemistry* 47 (20), S. 5565–5572. DOI: 10.1021/bi702036s.
- Powers, J. H. (2004). Antimicrobial drug development – the past, the present, and the future. In: *Clinical Microbiology and Infection* 10 (Supplement 4), S. 23–31. DOI: 10.1111/j.1465-0691.2004.1007.x.
- Pozo Navas, B.; Lohner, K.; Deutsch, G.; Sevcsik, E.; Riske, K. A.; Dimova, R. et al. (2005). Composition dependence of vesicle morphology and mixing properties in a bacterial model membrane system. In: *Biochimica et Biophysica Acta (BBA) - Biomembranes* 1716 (1), S. 40–48. DOI: 10.1016/j.bbamem.2005.08.003.
- Prossnigg, Florian; Hickel, Andrea; Pabst, Georg; Lohner, Karl (2010). Packing behaviour of two predominant anionic phospholipids of bacterial cytoplasmic membranes. In: *Biophysical Chemistry* 150 (1-3), S. 129–135. DOI: 10.1016/j.bpc.2010.04.004.
- Rappolt, Michael; Hickel, Andrea; Bringezu, Frank; Lohner, Karl (2003). Mechanism of the Lamellar/Inverse Hexagonal Phase Transition Examined by High Resolution X-Ray Diffraction. In: *Biophysical journal* 84 (5), S. 3111–3122. DOI: 10.1016/S0006-3495(03)70036-8.
- Rothman, J. E.; Lenard, J. (1977). Membrane asymmetry. In: *Science (New York, N.Y.)* 195 (4280), S. 743–753.
- Roversi, Daniela; Luca, Vincenzo; Aureli, Simone; Park, Yoonkyung; Mangoni, Maria Luisa; Stella, Lorenzo (2014). How many antimicrobial peptide molecules kill a bacterium? The case of PMAP-23. In: *ACS chemical biology* 9 (9), S. 2003–2007. DOI: 10.1021/cb500426r.

Scheinpflug, Kathi; Wenzel, Michaela; Krylova, Oxana; Bandow, Julia E.; Dathe, Margitta; Strahl, Henrik (2017). Antimicrobial peptide cWFW kills by combining lipid phase separation with autolysis. In: *Scientific reports* 7, S. 44332. DOI: 10.1038/srep44332.

Schibli, David J.; Epand, Raquel F.; Vogel, Hans J.; Epand, Richard M. (2002). Tryptophan-rich antimicrobial peptides. Comparative properties and membrane interactions. In: *Biochemistry and cell biology = Biochimie et biologie cellulaire* 80 (5), S. 667–677.

Sevcsik, E.; Pabst, G.; Richter, W.; Danner, S.; Amenitsch, H.; Lohner, K. (2008). Interaction of LL-37 with model membrane systems of different complexity: influence of the lipid matrix. In: *Biophys. J.* 94 (12), S. 4688–4699.

Shai, Yechiel; Oren, Ziv (2001). From “carpet” mechanism to de-novo designed diastereomeric cell-selective antimicrobial peptides. In: *Peptides* 22 (10), S. 1629–1641. DOI: 10.1016/S0196-9781(01)00498-3.

Shai, Yechiel (2002). Mode of action of membrane active antimicrobial peptides. In: *Biopolymers* 66 (4), S. 236–248. DOI: 10.1002/bip.10260.

Singer, S. J.; Nicolson, G. L. (1972). The fluid mosaic model of the structure of cell membranes. In: *Science (New York, N.Y.)* 175 (4023), S. 720–731.

Wang, Guangshun; Li, Xia; Wang, Zhe (2008). APD2. The updated antimicrobial peptide database and its application in peptide design. In: *Nucleic Acids Research* 37 (Database issue), D933–D937. DOI: 10.1093/nar/gkn823.

Wimley, William C. (2010). Describing the Mechanism of Antimicrobial Peptide Action with the Interfacial Activity Model. In: *ACS chemical biology* 5 (10), S. 905–917. DOI: 10.1021/cb1001558.

World Health Organization. (2014) Antimicrobial Resistance Global Report on Surveillance Summary. WHO. Geneva, Switzerland.

Zweytick, D.; Deutsch, G.; Andra, J.; Blondelle, S. E.; Vollmer, E.; Jerala, R.; Lohner, K. (2011). Studies on lactoferricin-derived Escherichia coli membrane-active peptides reveal differences in the mechanism of N-acylated versus nonacylated peptides. In: *J. Biol. Chem.* 286 (24), S. 21266–21276.